Journal of Rajasthan Academy of Physical Sciences
ISSN : 0972-6306; URL : http:/raops . org. in
Vol.13, No. 3 & 4, December, 2014, pp. 317-348

INFLUENCE OF HALL CURRENT ON CHEMICALLY REACTING MICROPOLAR FLUID FLOW FROM RADIATIVE ROTATING SURFACE WITH VARIABLE SUCTION AND SORET EFFECT IN SLIP-FLOW REGIME

R.C.CHAUDHARY
Department of Mathematics, University of Rajasthan, Jaipur-302004 (India)
E-mail: rcchaudhary@rediffmail.com,

PREETI JAIN
Department of Mathematics, Jagan Nath University,
NH-12, Rampura, Chaksu,, Jaipur-303 901 (India)
E-mail : jainpreeti28@rediffmail.com

Received : Nov. 5, 2014

Abstract : An analysis study is presented to study the effects of Hall current and Soret effect on unsteady hydromagnetic natural convection of a micropolar fluid in a rotating frame of reference with slip flow regime. A uniform magnetic field acts perpendicularly to the porous surface which absorbs the micropolar fluid with variable suction velocity. The effects of heat absorption, chemical reaction and thermal radiation are discussed and for this Rosseland approximation is used to describe the radiative heat flux in energy equation. The entire system rotates with uniform angular velocity Ω about an axis normal to the plate. The non-linear coupled partial differential equations are solved by perturbation techniques. In order to get physical insight, the numerical results of translational velocity, microrotation, fluid temperature and species concentration for different physical parameters entering into the analysis are discussed and explained graphically.

Key words : Hall Effect, Micropolar fluid, Soret effect, Chemical reaction, Rotation, MHD, Radiation, Heat absorption.

2010 Mathematical Subject Classification : 76A05, 76E06, 76R10, 76U05

1. Introduction

Micropolar fluids are subset of the micromorphic fluid. Micropolar fluids are those fluids consisting of randomly oriented particles suspended in a viscous medium, which can undergo a rotation that can affect the hydrodynamics of the flow, making it a distinctly non- Newtonian fluid. They constitute an important branch of non-Newtonian fluid dynamics where microrotation effects as well as micro inertia are exhibited. Modelling and analysis of the dynamics of micropolar fluids have been the field of very active research due to their application in a number of processes that occur in chemical, pharmaceutical and food industry. Such applications include the extrusion of polymer fluids, solidification of liquid crystals, cooling of a metallic plate in a bath, animal bloods, exotic lubricants and colloidal and suspension solutions, for example, for which the classical Navier-Stokes theory is inadequate. The essence of the theory of micropolar fluids lies in the extension of the constitutive equations for Newtonian fluids so that more complex fluids can be described by this theory. In this theory, rigid particles contained in a small fluid volume element are limited to rotation about the centre of the volume elements described by microrotation vector. It is well known that heterogeneous mixtures such as Ferro liquids, colloidal fluids, most slurries and suspensions, are some liquids with polymer activities, behave differently from Newtonian fluids. The main difference is that these types of fluids have a microstructure and exhibit micro-rotational effects and can support surface and body couples which are not present in the theory of Newtonian fluids. In order to study such types of fluids Eringen [9] developed the theory of micro fluids which include the effect of local rotary inertia, the couple stress and inertial spin. This theory is expected to be successful in analyzing the behavior of non-Newtonian fluids. Eringen [10] also developed the theory of micropolar fluids for the case where only microrotational effects and microrotational inertia exist. He [11] extended the theory of thermo micropolar fluids and derived the constitutive law for fluids with microstructure. An excellent review of micropolar fluids and their applications was given by Ariman et al. [1]. In view of Lukaszewicz [17], micropolar fluids represents those fluids which consist of randomly oriented particles suspended in a viscous medium.

Several authors have studied the characteristic of the boundary layer flow of micropolar fluid under different boundary conditions. Soundalgekar and Takhar [30, 31] studied the flow and heat transfer of micropolar fluid past a porous plate. Further, they [26, 32] discussed these problems past a continuously moving porous plate. Often experimental and analytical investigation of free convection flows are carried out by the researchers, since in many situations in technology and nature, one continually encounters masses of fluid arising freely in an extensive medium due to the buoyancy effects. Gorla et al. [12] investigated the natural convection from a heated vertical plate in micropolar fluid. The problem of flow and heat transfer for a micropolar fluid past a porous plate embedded in a porous medium has been of great use in engineering studies such as oil exploration, thermal insulation etc. Kim [16] have considered the micropolar fluid through a porous medium.

All the above mentioned studies are limited only to applications where radiative heat transfer is negligible. The role of thermal radiation in the flow heat transfer process is of great relevance in the design of many advanced energy conversion systems operating at higher temperatures. Nuclear power plants, gas turbines and the various propulsion devices for aircraft, missiles, satellites and space vehicles are examples of such engineering areas. Perdikis and Raptis. [19] illustrated the heat transfer of a micropolar fluid in the presence of radiation. Rahman and Satter [20] studied transient convective flow of micropolar fluid past a continuous moving porous plate in the presence of radiation. Moreover, when the radiative heat transfer takes place, the fluid involved can be electrically conducting in the sense that it is ionized owing to high operating temperature. Accordingly, it is of interest to examine the effect of the magnetic field on the flow. Thermal radiation effects on hydromagnetic natural convection flow with heat and mass transfer play an important role in manufacturing processes taking place in industries for the design of fins, glass production, steel rolling, casting and levitation, furnace design, etc. The process of fusing of metals in an electrical furnace by applying a magnetic field and the process of cooling of the first wall inside a nuclear reactor containment vessel where the hot plasma is isolated from the wall by applying a magnetic field are examples of such fields where thermal radiation and magnetohydrodynamics (MHD) are correlative. This fact was taken into consideration by Aziz [2] in his study on micropolar fluids. Raptis and Massalas [22] studied magneto hydrodynamic flow past a plate by the presence of radiation.

The rotating flow of an electrically conducting fluid in presence of magnetic field has got its importance in Geophysical problems. Investigation of hydromagnetic natural convection flow in a rotating medium is of considerable importance due to its application in various areas of geophysics, astrophysics and fluid engineering viz. maintenance and secular variations in Earth's magnetic field due to motion of Earth's liquid core, internal rotation rate of the Sun, structure of the magnetic stars, solar and planetary dynamo problems, turbo machines, rotating MHD generators, rotating drum separators for liquid metal MHD applications, etc. It may be noted that Coriolis and magnetic forces are comparable in magnitude and Coriolis force induces secondary flow in the flow-field. Changes that take place in the rotation, suggest the possible importance of hydro magnetic spin-up. Taking into consideration the importance of such study, unsteady hydromagnetic natural convection flow past a moving plate in a rotating medium is studied by Rapits and Singh [23]. This problem of spin-up in magneto hydrodynamic rotating fluids has been discussed under varied conditions by Takhar et al. [28].

The study of heat and mass transfer due to chemical reaction is also very importance because of its occurrence in most of the branches of science and technology. The processes involving mass transfer effects are important in chemical processing equipments which are designed to draw high value products from cheaper raw materials with the involvement of chemical reaction. Ibrahim and Makinde [13] investigated radiation effect on chemically reactive MHD boundary layer flow of heat and mass transfer past a porous vertical flat plate. Babu and Narayan [3] examined chemical reaction and thermal radiation effects on MHD convective flow in a porous medium in the presence of suction. Bakr [4] presented an analysis on MHD free convection and mass transfer adjacent to moving vertical plate for micropolar fluid in a rotating frame of reference in presence of heat generation /absorption and a chemical reaction using perturbation technique.

In all this study, the effect of Hall current is not considered. The current development of magnetohydrodynamics application is toward a strong magnetic field (so that the influence of electromagnetic force is noticeable) and toward a low density of the gas (such as in space flight and in nuclear fusion research). Under this condition, the Hall current becomes important. The rotating flow of an electrically conducting fluid in the presence of a magnetic field is encountered in cosmic fluid dynamics, medicine and biology. Application in biomedical engineering includes cardiac MRI, ECG, etc. MHD was pioneered Cowling [7] and he emphasized that when the strength of the applied magnetic field is sufficiently large, Ohm's law needs to be modified to include Hall current. The Hall Effect is merely due to the sideways magnetic force on the drafting free charges . Hall Effect results in a development of an additional potential difference between opposite surfaces of a conductor for which a current is induced perpendicular to both the electric and magnetic field. This current is termed as Hall current. Deka [8], Takhar et al. [29] have presented some model studies on the effect of Hall current on MHD convection flow because of its possible application in the problem of MHD generators and Hall current. Jain and Chaudhary [14] analyzed an unsteady hydromagnetic flow of a viscoelastic fluid from a radiative vertical porous plate, taking the effects of Hall current and mass transfer into account. Takhar et al. [27] investigated the simultaneous effects of Hall current and free stream velocity on the magneto hydrodynamic flow over a moving plate in a rotating fluid. When heat and mass transfer occur simultaneously in a moving fluid, the relations between the fluxes and the driven potential are important. It has been found that an energy flux can be generated not only by temperature gradients but by composition gradient as well. The energy caused by a composition gradient is called the Dufour or the diffusion-thermo effect, also the mass fluxes can also be caused by the temperature gradient and this is called the Soret or thermal diffusion effect i.e. if two regions in a mixture are maintained at different temperatures so that there is a flux of heat, it has been found that a concentration gradient is set up and in a binary mixture, one kind of a molecule tends to travel toward the hot region and the other kind toward the cold region. This is called the "Soret effect". The Dufour effect is neglected in this study because it is of a smaller order of magnitude than the magnitude of thermal radiation which exerts a stronger effect on the energy flux. Soret effects due to natural convection between heated inclined plates have been investigated by Raju et al. [21]. Reddy and Reddy [24] investigated Soret and Dufour effects on steady MHD free convective flow past an infinite plate. Practically, in many engineering applications, the particle adjacent to a solid surface no longer takes the velocity of the surface. The particle at the surface has a finite tangential velocity; it "slips" along the surface. This flow regime is called the slip-flow regime and this effect cannot be neglected. Jain and Chaudhary [15] examined the effects of radiation on the hydromagnetic free convection flow set up due to temperature as well as species concentration of an electrically conducting micropolar fluid past a vertical porous plate through porous medium in slip-flow regime. Chaudhary and Sharma [5] and Sharma [25] studied the free convection flow past a vertical porous plate with variable suction in slip-flow regime. Recently, Oahimire et al [18] investigated the effects of thermal-diffusion and thermal radiation on unsteady heat and mass transfer by free convective MHD micropolar fluid flow bounded by a semi- infinite vertical plate in a slip-flow regime under the action of transverse magnetic field with suction.

To the best of our knowledge, considerably less work has been done concerning the combined effect of Hall current and Soret effect on chemically reactive magneto-micropolar fluid flow incorporating the effect of rotation in slip flow regime in the presence of radiation and heat absorption. The results are in accordance with the physical realities which validate the correctness of our work presented here.

2. Mathematical formulation of the problem

Consider an unsteady hydromagnetic flow of an incompressible, viscous and electrically conducting micropolar fluid past an infinite vertical permeable plate embedded in a uniform porous medium in slip-flow regime and in a rotating system taking Hall current, thermal radiation, Soret effect and chemical reaction into account. The coordinate system is chosen in such a way that x^*-axis is considered along the porous plate in vertically upward direction, y^*-axis is taken along the width of the plate and z^*-axis normal to the plane of the plate in the fluid. Since the plate is infinite in extent in x* and y* directions, hence all physical quantities will be independent of x* and y* and they are functions of z* and t* only, that is $\frac{\partial u^*}{\partial x^*} = \frac{\partial u^*}{\partial y^*} = \frac{\partial v^*}{\partial x^*} = \frac{\partial v^*}{\partial y^*} = 0$,etc .

A magnetic field of uniform strength B_0 is applied in a direction parallel to z*-axis which is perpendicular to the flow direction. It is assumed that the induced magnetic field generated by fluid motion is negligible in comparison to the applied one. This assumption is justified because magnetic Reynolds number is very small for liquid metals and partially ionized fluids which are commonly used in industrial applications [6]. It is assumed that there is no applied or polarized voltage so the effect of polarization of fluid is negligible. This corresponds to the case where no energy is added or extracted from the fluid by electrical means. The entire system is rotating with an angular velocity Ω about the normal to the plate. It is assumed here that the hole size of the porous plate is significantly larger than the characteristic microscopic length scale of the porous medium. The fluid is considered to be a gray, absorbing-emitting but non-scattering medium and the Rosseland approximation is used to describe the radiative heat flux. The radiative heat flux in the x*-direction is considered negligible in comparison with that of z*-direction. When the strength of the magnetic field is very large, the generalized Ohm's law in the absence of electric field takes the following form:

$$\vec{J} + \frac{\omega_e \tau_e}{B_0} \vec{J} \times \vec{H} = \sigma\left(\mu_e \vec{V} \times \vec{H} + \frac{1}{en_e} \nabla P_e\right)$$

Under the assumption that the electron pressure (for weakly ionized gas), the thermo-electric pressure and ion-slip conditions are negligible, now the above equation becomes:

$$j_x = \frac{\sigma \mu_e H_0}{1+m^2}(mv-u) \text{and}\, j_z = \frac{\sigma \mu_e H_0}{1+m^2}(mu+v)$$

where u is the x-component of $\vec{V}$, v is the y-component of $\vec{V}$ and m $(=\omega_e \tau_e)$ is Hall parameter.

The suction velocity is assumed to be, $w^* = -w_0(1+\varepsilon A e^{\delta^* t^*})$ where ε and εA are small values less than unity and w_0 is the scale of suction velocity which is non-zero positive constant. The negative sign indicates that the suction is towards the plate. The fluid properties are assumed to be constants except that the influence of density variation with temperature and concentration has been considered in the body-force term. There is a first order chemical reaction between the diffusing species and the fluid.

With these foregoing assumptions, the governing equations under Boussinesq approximation can be written in a Cartesian frame of reference as follows:

(a) Continuity

$$\frac{\partial w^*}{\partial z^*} = 0 \qquad \ldots(1)$$

(b) Linear Momentum

$$\frac{\partial u^*}{\partial t^*} + w^* \frac{\partial u^*}{\partial z^*} - 2\Omega v^* = (\nu + \nu_r)\frac{\partial^2 u^*}{\partial z^{*2}} + g\beta_T (T - T_\infty) + g\,\beta_C (C^* - C^*_\infty) - \frac{\nu u^*}{K^*} - \nu_r \frac{\partial \omega_2^*}{\partial z^*} + \frac{\sigma \mu_e^2 H_0^2 (m v^* - u^*)}{\rho(1+m^2)} \qquad \ldots(2)$$

$$\frac{\partial v^*}{\partial t^*} + w^* \frac{\partial v^*}{\partial z^*} + 2\Omega u^* = (\nu + \nu_r)\frac{\partial^2 v^*}{\partial z^{*2}} - \frac{\nu u^*}{K^*} + \nu_r \frac{\partial \omega_1^*}{\partial z^*} - \frac{\sigma \mu_e^2 H_0^2 (m u^* + v^*)}{\rho(1+m^2)} \qquad \ldots(3)$$

© Angular momentum

$$\frac{\partial \omega_1^*}{\partial t^*} + w^* \frac{\partial \omega_1^*}{\partial z^*} = \frac{\Lambda}{\rho j}\frac{\partial^2 \omega_1^*}{\partial z^{*2}} \qquad \ldots(4)$$

$$\frac{\partial \omega_2^*}{\partial t^*} + w^* \frac{\partial \omega_2^*}{\partial z^*} = \frac{\Lambda}{\rho j}\frac{\partial^2 \omega_2^*}{\partial z^{*2}} \qquad \ldots(5)$$

(d) Energy

$$\frac{\partial T}{\partial t^*} + w^* \frac{\partial T}{\partial z^*} = \frac{k}{\rho C_p}\frac{\partial^2 T}{\partial z^{*2}} - \frac{Q^*}{\rho C_p}(T - T_\infty) - \frac{1}{\rho C_p}\frac{\partial q_r}{\partial z^*} \qquad \ldots(6)$$

(e) Mass transfer

$$\frac{\partial C^*}{\partial t^*} + w^* \frac{\partial C^*}{\partial z^*} = D_m \frac{\partial^2 C^*}{\partial z^{*2}} + \frac{D_m K_t}{T_m} \frac{\partial^2 T^*}{\partial z^{*2}} - R_C (C^* - C^*_\infty) \qquad \ldots(7)$$

The initial and boundary conditions suggested by the physics of the problem are:

$$u^* = v^* = 0, \quad \omega_1^* = \omega_2^* = 0, \quad T = T_\infty, \quad C^* = C^*_\infty \quad \text{for} \quad t^* \le 0 \qquad \ldots(8)$$

$$\left.\begin{array}{ll} u^* = U_r + L^* \left(\frac{\partial u^*}{\partial z^*}\right), v^* = 0, \omega_1^* = -\frac{1}{2}\frac{\partial v^*}{\partial z^*}, \omega_2^* = \frac{1}{2}\frac{\partial u^*}{\partial z^*}, T = T_w, C^* = C^*_w & \text{at } z^* = 0 \\ u^* \to 0,\ v^* \to 0,\ \omega_1^* \to 0,\ \omega_2^* \to 0,\ T \to T_\infty,\ C^* \to C^*_\infty & \text{as } z^* \to \infty \end{array}\right\} \text{for } t^* > 0$$

$$\ldots(9)$$

The boundary condition for microrotation components ω_1^* and ω_2^* describe its relationship with the surface stress. In the above boundary condition (9) the plate is in uniform motion and subjected to variable suction and slip boundary condition. In the parameter $L^* = \left(\frac{2 - m_1}{m_1}\right) L$, L is the molecular mean free path and m_1 is the tangential momentum accommodation coefficient. All the physical variables are given in nomenclature.

Integration of continuity equation (1) for variable suction velocity normal to the plate gives $w^* = -\ w_0 (1 + \in A\ e^{\delta^* t^*})$ $\ldots(10)$

here w_0 represents the normal velocity at the plate which is positive for suction and negative for blowing. The radiative heat flux term by using Rosseland approximation is given by:

$$q_r = -\frac{4\sigma^*}{3a_R} \frac{\partial T^4}{\partial z^*} \qquad \ldots(11)$$

We assume that the temperature differences within the flow are such that T^4 may be expressed as a linear function of the temperature T. This is accomplished by expanding T^4 in a Taylor series about T_∞ and neglecting higher order terms, we have

$$T^4 \simeq 4T_\infty^3\, T - 3T_\infty^4 \qquad \dots(12)$$

By using equations (11) and (12), equation (6) gives

$$\frac{\partial T}{\partial t^*} + w^* \frac{\partial T}{\partial z^*} = \frac{k}{\rho C_p}\frac{\partial^2 T}{\partial z^{*2}} - \frac{Q^*}{\rho C_p}(T - T_\infty) + \frac{16\sigma^* T_\infty^3}{3\rho C_p a_R}\frac{\partial^2 T}{\partial z^{*2}} \qquad \dots(13)$$

Proceeding with analysis, we introduce the following dimensionless variables:

$$u = \frac{u^*}{U_r},\ v = \frac{v^*}{U_r},\ z = \frac{z^* U_r}{\nu},\ t = \frac{t^* U_r^2}{\nu},\ \delta = \frac{\delta^* \nu}{U_r^2}, \omega_1 = \frac{\omega_1^* \nu}{U_r^2}, \omega_2 = \frac{\omega_2^* \nu}{U_r^2}$$

$$Gr = \frac{\nu g\beta_T (T_w - T_\infty)}{U_r^3},\ Gc = \frac{\nu g\beta_C (C_w^* - C_\infty^*)}{U_r^3},\ R = \frac{2\Omega \nu}{U_r^2},\ S = \frac{w_0}{U_r},\ \Delta = \frac{\nu_r}{\nu}$$

$$\theta = \frac{T - T_\infty}{T_w - T_\infty},\ C = \frac{C^* - C_\infty^*}{C_w^* - C_\infty^*},\ K = \frac{K^* U_r^2}{\nu^2},\ M = \frac{\mu_e H_0}{U_r}\sqrt{\frac{\sigma \nu}{\rho}},\ \lambda = \frac{\Lambda}{\mu j},\ Pr = \frac{\mu C_p}{k},$$

$$Sc = \frac{\nu}{D_m}\ F = \frac{4T_\infty^3 \sigma^*}{k a_R},\ Q = \frac{Q^* \nu^2}{U_r^2 k},\ Sr = \frac{D_m K_t (T_W - T_\infty)}{T_m (C_W^* - C_\infty^*)\nu}, \alpha = \frac{R_C \nu}{U_r^2},$$

$$h = \frac{L^* U_r}{\nu} \qquad \dots(14)$$

In view of equation (14), the governing equations (2) - (7) and equation (13) reduce to the following dimensionless form:

$$\frac{\partial u}{\partial t} - S(1 + \varepsilon A e^{\delta t})\frac{\partial u}{\partial z} - Rv = (1+\Delta)\frac{\partial^2 u}{\partial z^2} + Gr\theta + Gm\phi - \left(\frac{M^2}{1+m^2} + \frac{1}{k}\right)u - \Delta\frac{\partial \omega_2}{\partial z} + \frac{mM^2}{1+m^2}v \qquad \dots(15)$$

$$\frac{\partial v}{\partial t} - S(1+\varepsilon A e^{\delta t})\frac{\partial v}{\partial z} + Ru = (1+\Delta)\frac{\partial^2 v}{\partial z^2} - \left(\frac{M^2}{1+m^2}+\frac{1}{k}\right)v + \Delta\frac{\partial \omega_1}{\partial z} - \frac{mM^2}{1+m^2}u \quad \ldots(16)$$

$$\frac{\partial \omega_1}{\partial t} - S(1+\varepsilon A e^{\delta t})\frac{\partial \omega_1}{\partial z} = \lambda\frac{\partial^2 \omega_1}{\partial z^2} \quad \ldots(17)$$

$$\frac{\partial \omega_2}{\partial t} - S(1+\varepsilon A e^{\delta t})\frac{\partial \omega_2}{\partial z} = \lambda\frac{\partial^2 \omega_2}{\partial z^2} \quad \ldots(18)$$

$$\frac{\partial \theta}{\partial t} - S(1+\varepsilon A e^{\delta t})\frac{\partial \theta}{\partial z} = \frac{1}{Pr}\left(1+\frac{4F}{3}\right)\frac{\partial^2 \theta}{\partial z^2} - \frac{Q}{Pr}\theta \quad \ldots(19)$$

$$\frac{\partial C}{\partial t} - S(1+\varepsilon A e^{\delta t})\frac{\partial C}{\partial z} = \frac{1}{Sc}\frac{\partial^2 C}{\partial z^2} + Sr\frac{\partial^2 C}{\partial z^2} - \alpha C \quad \ldots(20)$$

The boundary conditions (8)-(9) in view of eq. (14) is then given by the following dimensionless form:

$$u = v = 0,\ \omega_1 = \omega_2 = 0,\ \theta = 0,\ C = 0 \quad \text{for} \quad t \le 0 \quad \ldots(21)$$

$$\left.\begin{array}{ll} u = 1 + h\dfrac{\partial u}{\partial z},\ v=0,\ \omega_1 = -\dfrac{1}{2}\dfrac{\partial v}{\partial z},\ \omega_2 = \dfrac{1}{2}\dfrac{\partial u}{\partial z}, \theta = 1,\ C = 1 & \text{at } z = 0 \\ u \to 0,\ \omega_1 \to 0,\ \omega_2 \to 0,\ \theta \to 0,\ C \to 0 & \text{as } z \to \infty \end{array}\right\} \text{for } t > 0 \quad \ldots(22)$$

To simplify equations (15) - (18), we substitute the fluid velocity and angular velocity in the complex form as $V = u + iv$, $\omega = \omega_1 + i\omega_2$ and we get:

$$\frac{\partial V}{\partial t} - S(1+\varepsilon A e^{\delta t})\frac{\partial V}{\partial z} + iRV = (1+\Delta)\frac{\partial^2 V}{\partial z^2} + Gr\theta + Gm\phi - \left(\frac{M^2}{1+m^2}+\frac{1}{k}\right)V - i\Delta\frac{\partial \omega}{\partial z} - i\left(\frac{mM^2}{1+m^2}\right)V \quad \ldots(23)$$

$$\frac{\partial \omega}{\partial t} - S(1+\varepsilon A e^{\delta t})\frac{\partial \omega}{\partial z} = \lambda\frac{\partial^2 \omega}{\partial z^2} \quad \ldots(24)$$

The associated boundary conditions (21) and (22) become:

$$\left.\begin{array}{l} V=0,\ \ \omega=0,\ \ \theta=0,\ \ C=0 \quad \text{for} \quad t\le 0 \\ V=1+h\dfrac{\partial u}{\partial z},\ \omega=\dfrac{i}{2}\dfrac{\partial V}{\partial z},\ \theta=1,\ C=1 \quad \text{at}\ z=0 \\ V\to 0,\ \omega\to 0,\ \theta\to 0,\ C\to 0 \quad \text{as}\ z\to\infty \end{array}\right\}\text{for}\ t>0 \qquad \ldots(25)$$

3. Analytical solution of the problem :

In order to reduce the above system of partial differential equations to a system of ordinary differential equations in dimensionless form, we represent the translational velocity V, microrotation velocity ω, temperature θ and concentration C as:

$$V(z,t) = V_0(z) + \varepsilon\, e^{\delta t} V_1(z) + O(\varepsilon^2) \qquad \ldots(26)$$

$$\omega(z,t) = \omega_0(z) + \varepsilon\, e^{\delta t} \omega_1(z) + O(\varepsilon^2) \qquad \ldots(27)$$

$$\theta(z,t) = \theta_0(z) + \varepsilon\, e^{\delta t} \theta_1(z) + O(\varepsilon^2) \qquad \ldots(28)$$

$$C(z,t) = C_0(z) + \varepsilon\, e^{\delta t} C_1(z) + O(\varepsilon^2) \qquad \ldots(29)$$

By substituting the above equations (26) – (29) into equations (19), (20), (23) - (25) and equating the harmonic and non-harmonic terms and neglecting the higher-order terms of $O(\varepsilon^2)$, we obtain The expression for translational velocity V, microrotation velocity ω, temperature θ and concentration C as:

$$V(z,t) = B_{11}e^{-r_5 z} + B_8 e^{-r_1 z} + B_9 e^{-r_3 z} + B_{10} e^{-\frac{S}{\lambda}z} + \varepsilon e^{\delta t}\Big\{B_{20}e^{-r_7 z} + B_{13}e^{-r_1 z} + B_{14}e^{-r_2 z} + B_{15}e^{-r_4 z} + B_{16}e^{-r_3 z} + B_{17}e^{-r_5 z} + B_{18}e^{-\frac{S}{\lambda}z} + B_{19}e^{-r_6 z}\Big\} \qquad \ldots(30)$$

$$\omega(z,t) = D_1 e^{-\frac{S}{\lambda}z} + \varepsilon e^{\delta t}\left\{D_2 e^{-r_6 z} + B_{12} e^{-\frac{S}{\lambda}z}\right\} \qquad \ldots(31)$$

$$\theta(z,t) = e^{-r_1 z} + \varepsilon e^{\delta t}\left\{B_1\left(e^{-r_1 z} - e^{-r_2 z}\right)\right\} \qquad \ldots(32)$$

$$C(z,t) = B_3 e^{-r_3 z} + B_2 e^{-r_1 z} + \varepsilon e^{\delta t}\left\{B_4 e^{-r_3 z} + B_5 e^{-r_1 z} + B_6 e^{-r_2 z} + B_7 e^{-r_4 z}\right\} \qquad \ldots(33)$$

In technological applications, the wall shear stress, the wall couple stress and the heat and mass transfer rate are often of great interest. Skin friction is caused by viscous drag in the boundary layer around the plate. The skin friction coefficient (C_f) at the wall in dimensionless form is given by:

$$C_f = \frac{\tau_w^*\big|_{z^*=0}}{\rho U_r^2} = \left\{1 + \Delta\left(1 + \frac{i}{2}\right)\right\}\frac{\partial V}{\partial z}\bigg|_{z=0} \qquad \ldots(34)$$

$$= -\left\{1 + \Delta\left(1 + \frac{i}{2}\right)\right\}\left\{B_{11} r_5 + B_8 r_1 + B_9 r_3 + B_{10}\frac{S}{\lambda} + \varepsilon\, e^{\delta t}\left(B_{20} r_7 + B_{13} r_1 + B_{14} r_2 + B_{15} r_4 + B_{16} r_3 + B_{17} r_5 + B_{18}\frac{S}{\lambda} + B_{19} r_6\right)\right\} \qquad \ldots(35)$$

The couple stress coefficient (C_m) at the plate is defined by:

$$M_w = \Lambda \frac{\partial \omega^*}{\partial z^*}\bigg|_{z^*=0} \qquad \ldots(36)$$

and in the dimensionless form it is given by:

$$C_m = \frac{M_w}{\mu j U_r} = \left(1 + \frac{\Delta}{2}\right)\frac{\partial \omega}{\partial z}\bigg|_{z=0} = \left(1 + \frac{\Delta}{2}\right)\left\{\frac{\partial \omega_1}{\partial z}\bigg|_{z=0} + i\frac{\partial \omega_2}{\partial z}\bigg|_{z=0}\right\} \qquad \ldots(37)$$

$$= -\left(1+\frac{\Delta}{2}\right)\left\{D_1\frac{S}{\lambda}+\varepsilon e^{\delta t}\left(D_2 r_6 + B_{12}\frac{S}{\lambda}\right)\right\} \qquad \ldots(38)$$

Knowing the temperature field, it is interesting to study the effect of the free convection and thermal radiation on the rate of heat transfer and this is given by:

$$q_w^* = -k\frac{\partial T}{\partial z^*} - \frac{4\sigma^*}{3a_R}\left(\frac{\partial T^4}{\partial z^*}\right)\Bigg|_{z^*=0} \qquad \ldots(39)$$

Using $T^4 \simeq 4T_\infty^3 T - 3T_\infty^4$ the above equation becomes,

$$q_w^* = -k\left(T_w - T_\infty\right)\frac{U_r}{\nu}\left(1+\frac{4F}{3}\right)\frac{\partial\theta}{\partial z}\Bigg|_{z=0} \qquad \ldots(40)$$

The rate of heat transfer between the fluid and the plate is studied in terms of non-dimensional Nusselt number, which is given by:

$$Nu = \frac{x\,q_w^*}{k\left(T_w - T_\infty\right)} = -Re_x\left(1+\frac{4F}{3}\right)\frac{\partial\theta}{\partial z}\Bigg|_{z=0} \qquad \ldots(41)$$

where $Re_x = \dfrac{U_r x}{\nu}$ is the local Reynolds number.

$$\begin{aligned} Nu\,Re_x^{-1} &= \left(1+\frac{4F}{3}\right)\frac{\partial\theta}{\partial z}\Bigg|_{z=0} \\ &= \left(1+\frac{4F}{3}\right)\left\{r_1 + \varepsilon e^{\delta t}\left[B_1(r_1 - r_2)\right]\right\} \end{aligned} \qquad \ldots(42)$$

The definitions of the local mass flux and the local Sherwood number are respectively given by:

$$j_w = -D_m\frac{\partial C^*}{\partial z^*}\Bigg|_{z^*=0} \qquad \ldots(43)$$

$$Sh_x = \frac{j_w\ x}{D_m(C_w^* - C_\infty^*)} = -Re_x \left.\frac{\partial C}{\partial z}\right|_{z=0} \quad \ldots(44)$$

$$Sh_x\, Re_x^{-1} = \left.\frac{\partial C}{\partial z}\right|_{z=0} = B_3 r_3 + B_2 r_1 + \varepsilon e^{\delta t}\left(B_4 r_3 + B_5 r_1 + B_6 r_2 + B_7 r_4\right) \ldots(45)$$

4. Results and Discussion:

In the preceding sections, the governing equations along with the boundary conditions are solved analytically employing the perturbation techniques. The effects of main controlling parameters as they appear in the governing equations are discussed on the temperature θ, concentration C, translational velocity V, microrotation ω. In order to get a physical insight of the problem the above physical quantities are complied numerically and displayed graphically. In the entire calculations we have chosen $\varepsilon = 0.01, \delta = 0.1, t = 1$ and $A = 1$ while Pr, S, F, Q, Sr, Sc, M, m, Gr, Gm, R, h, K, Δ and λ are varied over the range which are listed in the figure legends.

The numerical values of fluid temperature θ computed from the analytical solutions (eq. no. 40) are illustrated graphically versus boundary layer coordinate z in Fig.1 for various values of Prandtl number (Pr), Suction parameter (S), Heat absorption parameter (Q) and radiation parameter (F).The values of Prandtl number are chosen as Pr = 0.71, 0.025, and 7.0 which physically correspond to air, mercury and water at 25^o temperature and one atmospheric pressure. Pr = 11.62 correspond to water at 4^oC. It is inferred that the temperature falls more rapidly for water in comparison to air which is physically true thus the thermal boundary layer falls quickly for large value of Prandtl number. The thickness of thermal boundary layer is greatest for Pr = 0.025 (Mercury) than for Pr = 0.71 (Air), thereafter for Pr = 7 (Water) and finally lowest for Pr = 11.62 (water at 4^0 C) i.e. an increase in Prandtl number results in a decrease of temperature. The reason underlying such a behavior is that Pr signifies the relative effects of viscosity to thermal conductivity and smaller values of Prandtl number posses high thermal conductivity and therefore heat is able to diffuse away from the surface faster than at higher values of Pr. This results in the reduction of thermal boundary layer thickness. The fluid temperature θ also decreases with an increase of Heat absorption parameter (Q) and Suction parameter (S). The effect of thermal radiation parameter (F) is to enhance the fluid temperature throughout the boundary layer region. Thus it is pointed out that radiation should be minimized to have the cooling process at a faster rate. The temperature profiles attain their maximum value at the wall and decrease exponentially with z and finally tend to zero as $z \to \infty$. Hence the accuracy is checked and it validates that the analytical results for temperature is correct.

Graphical results of concentration profiles C for different values of Schmidt number (Sc) and Chemical reaction parameter (α) are displayed in Fig. 2(a). The values of Schmidt number are chosen to represent the most common diffusing chemical species which are of interest and they are Sc = 0.22 (Hydrogen), Sc = 0.3 (Helium), Sc = 0.6 (water vapor), Sc = 0.94 (carbon dioxide) and Sc = 2.62 (Propyl Benzene) at 25 ^{0}C temperature and one atmospheric pressure. A comparison of curves in the figure show the concentration distribution decreases at all points in the flow field with an increase in Schmidt number because smaller values of Sc are equivalent to increasing Chemical molecular diffusivity (D). This implies mass diffusion tends to enhance species concentration. Furthermore, it is interesting to note that concentration profiles fall slowly and steadily for Hydrogen (Sc = 0.22) and Helium (Sc = 0.30) but falls very rapidly for water vapor (Sc = 0.6) and Propyl Benzene (Sc = 2.62). Further, this figure clearly demonstrates that the concentration profiles decrease rapidly when chemical reaction parameter is increased this is due to the fact that boundary layer decreases with an increase in the value of α in this system, results in the consumption of the chemical and hence result in decreasing concentration profile. Thus the diffusion rates can be tremendously altered by chemical reaction.

The effects of heat absorption parameter (Q) and Soret number (Sr) on concentration profiles across the boundary layer are displayed in Fig. 2(b). The results show that solutal boundary layer suppresses with an increase in heat absorption parameter and Soret number. The profiles fall rapidly with an increase of Soret number and thereafter increase and tend to zero as $z \to \infty$. Fig. 2(c) is plotted to show the effects of radiation parameter (F) and Suction parameter (S) on the species concentration profiles. It is revealed that the presence of Suction parameter diminishes the concentration distribution where as reverse phenomena is observed with increasing values of radiation parameter. In Figs. 2(a) - 2(c) the concentration profiles attain their maximum value at the wall and decrease exponentially with z and finally tend to zero as $z \to \infty$. The micro rotation profiles (ω) against span wise coordinate z incorporating the effect of various parameters influencing the flow field are demonstrated in Fig. 3(a) - 3(h). It is revealed from Figs. 3(a) - 3(h) that these profiles attain a distinctive maximum value near surface of the plate and decrease properly on increasing boundary layer coordinate z to approach free stream value. Fig. 3(a) shows the influence of Prandtl number (Pr), Suction parameter (S) and radiation parameter (F) on micro rotation profiles. It is noticed that micro rotation profiles (ω) decrease on increasing Pr. This figure further indicates that the micro rotation profiles decrease with an increase in suction parameter (S) because sucking decelerates the fluid particles through the porous wall and hence reduce the growth of the fluid boundary layer as well as thermal and concentration boundary layers. These profiles enhances with an increase in radiation parameter (F).

From Fig.3 (b) it is perceived that micro rotation profiles decrease with an increase in heat absorption parameter (Q). Fig. 3(c) elucidate the influence of magnetic parameter (M) and Hall parameter (m) on micro rotation profiles (ω), it is clear from these curves that these profiles increase when magnetic parameter and Hall current parameter are increased. The profiles corresponding to m = 0 reveals that micro elements close to the wall are unable to rotate hence ω is very small. Fig. 3(d) demonstrate the effect of thermal and concentration buoyancy forces i.e. Grashof number (Gr) and modified Grashof number (Gm) on the micro rotation profiles. Here the negative value of Grashof number (Gr < 0), physically corresponds to heating of the plate while the positive value (Gr > 0) represents cooling of the plate. Hence, it is observed from the comparison of the curves that an increase in thermal Grashof number leads to an increase in the velocity due to an enhancement in buoyancy forces. Furthermore, the comparison of the curves illustrate that velocity increases with increasing Gm. The profiles attain a maximum value near the wall and then decrease rapidly to approach the free stream value. For various values of rotational parameter (R), the profiles of micro rotation across the boundary layer are shown in Fig. 3(e). It is perceived that the rotation tend to decrease the microtation profiles. Fig. 3(f) presents the effect of viscosity ratio (Δ) and material parameter (λ) on ω. The magnitude of micro rotation is greater for a Newtonian fluid ($\Delta = 0$) with given parameters as compared with micropolar fluids ($\Delta \neq 0$)**.** Also, it is observed that the magnitude of micro rotation profiles decrease with an increase in material parameter (λ) and viscosity ratio (Δ).The microtation profiles presented in Fig. 3(g) incorporate the influence of rarefaction parameter (h) and permeability parameter (K). It is noticed that an increase in the value of rarefaction parameter decrease the magnitude of microtation profiles while the comparison of curves for different values of permeability parameter (K) reflects that profiles increase with increasing values of K.

Microtation profiles showing the variation of Soret parameter (Sr), Schmidt number (Sc) and generative chemical reaction (α) are presented in Fig. 3 (h). It is analyzed that the influence of Sr, Sc and α is to reduce the magnitude of microtation profiles. Comparison of the curves in this figure indicate that the magnitude of microtation profiles is greatest for Helium (He: Sc = 0.3) and then for Carbon dioxide (CO_2: Sc = 0.94) and lowest for Propyl Benzene (C_9H_{10}: Sc = 2.62). Physically it is justified because for large value of Schmidt number, the fluid becomes denser. This figure also displays the fact that these profiles decrease during the destructive reaction ($\alpha > 0$).

Figs. 4(a) - 4(h) illustrate graphically the behavior of translational velocity (V) versus boundary layer coordinate z for various involved parameters governing the flow field. For various values of Prandtl number (Pr), Suction parameter (S) and Radiation

Parameter (F), the profiles of translational velocity across boundary layer are shown in Fig. 4(a). It is clearly evident that translational velocity decrease on increasing Pr Moreover, it is noticed that velocity first increases in the region adjacent to the plate and then decreases on moving away from the plate with increase in the suction parameter (S) showing the suction has a stabilizing effect on the flow field. This figure also incorporates the fact that radiation (F) tends to accelerate the translational velocity throughout the boundary layer region. The velocity distribution attains maximum value in the neighborhood of the wall and then decrease to approach the free stream value. The effect of heat absorption parameter on translational velocity (V) is depicted in Fig.4 (b) and it is found that velocity reduces due to the presence of heat absorption parameter (Q).

Fig. 4(c) incorporates the influence of magnetic parameter (M) and hall parameter (m) on the translational velocity profiles (V). As expected, the application of the transverse magnetic field retards the fluid motion. As such the magnetic field is an effective regulatory mechanism for the flow regime. Form this figure it is also found that hall currents (m) tends to accelerate the fluid velocity throughout the boundary layer region which is consistent with the fact that Hall currents induces flow in the flow field.

The combined effect of thermal and concentration buoyancy forces on the translational velocity are depicted in Fig.4 (d). It is evident from this figure that with an increase in Grashof number (Gr) and modified Grashof number (Gm), which is a measure of thermal and concentration buoyancy forces; there is a substantial growth in the momentum boundary layer for the same reasons as explained earlier in this section. Fig. 4(e) depicts the effect of rotational parameter (R) on the fluid velocity and it is perceived that rotation tends to retard fluid velocity throughout the flow field. This is due to the reason that Coriolis force is dominant in the region near to the axis of rotation.

Variation of translational velocity profiles for different values of Soret parameter (Sr), Schmidt number (Sc) and chemical reaction (α) are displayed in Fig. 4(f).The comparison of the curves show that the velocity of the flow field decreases due to an increase in Schimdt number and Soret number. It is also observed from this figure that velocity decreases during the destructive reaction ($\alpha < 0$).

Fig. 4(g) depicts the influence of viscosity ratio (Δ) and permeability parameter (K) on the translational velocity (V). For different values of permeability parameter this figure shows that velocity increases with increasing values of K while an increasing viscosity ratio (Δ) results in an enhancement of the total viscosity in fluid flow because Δ is directly proportional to vortex viscosity which makes the fluid more viscous and so weaken the convection currents and hence the velocity decreases. This phenomenon has a good agreement with the physical realities.

Fig. 4(h) incorporates the effect of slip or rarefaction parameter (h) and material parameter (λ) on the translational velocity (V). It is observed that an increase in the values of rarefaction parameter result in an enhancement of the flow field inside the boundary layer. This behavior is readily understood from the velocity slip condition at the surface (eq. no. 25). The case when h = 0 corresponds to the no slip condition and in the present case it reduces to the case when the plate moves with constant velocity in the longitudinal direction. The effects are more visible in the region near to the plate and afterwards it fall slowly and steadily to its free stream value as $z \to \infty$. Lastly the velocity decreases with increasing material parameter (λ). In Figs. 4(a) - 4(h) we observe that the velocity become maximum in the vicinity of the plate and then decreases away from the plate and finally takes asymptotic values far away from the plate.

Nomenclature

a_R	Rosseland mean absorption coefficient
A	Positive constant
B_0	Applied magnetic field
C	Concentration of the solute in dimensionless form
C^*	Concentration of the solute in the fluid
C_w^*	Concentration of the solute near the plate
C_∞^*	Concentration of the solute far away from the plate
C_p	Specific heat at constant pressure
C_f	Skin-friction coefficient
C_m	Couple stress coefficient
D_m	Chemical molecular diffusivity
en_e	Electron charger
F	Radiation parameter
g	Acceleration due to gravity
Gr	Grashof number
Gm	Modified Grashof number
h	Rarefaction parameter
$\vec{H}$	Magnetic field strength
H_0	Externally applied transverse magnetic field
i	Imaginary unit
j	Microinertia density
$\vec{J}$	Current strength
K^*	Permeability of the porous medium
K	Non-dimensional permeability of the porous medium
k	Thermal conductivity of the fliud

K_T	Thermal diffusion ratio
M	Magnetic parameter
m	Hall parameter
n_e	Number density of the electron
P_e	Electron pressure
Pr	Prandtl number
Q	Heat absorption parameter
q_r	Radiative heat flux
R	Rotational parameter
R_C	Chemical reaction rate constant
S	Suction parameter
Sc	Schmidt number
Sr	Soret number
t	Dimensionless time
t^*	Time
T_m	Mean fluid temperature
T	Temperature of the fluid near the plate
T_w	Temperature of the plate
T_∞	Temperature of the fluid far away from the plate
U_r	Plate velocity in the direction of flow
$\vec{V}$	Velocity vector
(u^*, v^*, w^*)	Components of dimensional velocities along x^*, y^* and z^* direction respectively
(u, v w)	Dimensionless velocities along x, y and z direction respectively
(x^*, y^*, z^*)	Cartesian coordinates
(x, y, z)	Dimensionless Cartesian coordinates

Greek symbol

δ	Exponential index
δ^*	Dimensionless exponential index
α	Chemical reaction parameter
β_T	Coefficient of volumetric thermal expansion of the fluid
β_C	Volumetric Coefficient of expansion with concentration
Δ	Dimensionless viscosity ratio
ν	Kinematic viscosity
ν_r	Kinematic rotational viscosity
Λ	Spin- gradient viscosity
Ω	Angular velocity
λ	Dimensionless material parameter
μ	Coefficient of viscosity
μ_e	Magnetic permeability
σ	Electrical conductivity of the fluid
σ^*	Stefan-Boltzmann constant
ρ	Density of the fluid

τ_e Electron collision time
ω_e Electron frequency
(ω_1, ω_2) Microrotation components
ω Dimensionless microrotation profile
θ Dimensionless temperature of the plate

References

[1] Ariman, T. M. A. *Turk, and N. D. Sylvester (1973).* Microcontinuum fluid mechanics: a review, *International Journal of Engineering Science,* **11 (8)**, 905–930.

[2] Aziz M. Abd-El (2006). Thermal radiation effects on magnetohydro-dynamic mixed convection flow of a micropolar fluid past a continuously moving semi-infinite plate for high temperature differences, *Acta Mechanica,* **187**, 113-127.

[3] Babu M. S. and Satya Narayan P. V. (2009). Effects of the chemical reaction and radiation absorption on free convection flow through porous medium with variable suction in the presence of uniform magnetic field, *Journal of Heat and Mass Transfer*, **3**, 219–234.

[4] Bakr A.A. (2011). Effects of chemical reaction on MHD free convection and mass transfer flow of a micropolar fluid with oscillatory plate velocity and onstant heat source in a rotating frame of reference, *Communication in Nonlinear Science and Numerical Simulation*, **16**, 698-710.

[5] Chaudhary R.C. and Sharma P.K. (2003). Effect of variable suction in transient free convection viscous incompressible flow past a vertical plate with periodic temperature variations in slip flow regime, *Emirates Journal for Engineering Research,* **8**, 33-38.

[6] Cramer K. R. and Pai S. I. (1973). *Magnetofluid Dynamics for Engineers and Applied Physicists,* McGraw Hill Book Company, New York.

[7] Cowling T. G. (1957). *Magnet Hydrodynamics,* Wiley Inter Science, New York.

[8] Deka R. K. (2008). Hall effects on MHD flow past an accelerated plate, *Theoretical and Applied Mechanics,* **35 (4)**, 333-346,

[9] Eringen A.C. (1964). Simple micro fluids, *International Journal of Engineering Science,* **2**, 205-217.

[10] Eringen A.C. (1966). Theory of Micropolar Fluids, *Journal of Mathematical Fluid Mechanics,* **16**, 1-18.

[11] Eringen A.C. (1972): Theory of Thermomicrofluids, *Journal of Mathematical Analysis and Applications,* .**38**, 480-496.

[12] Gorla R. S. R., Mohammedan A., Mansour M. and Hussein I. (1995). Unsteady natural convection from a heated vertical plate in micropolar fluid, *Numerical Heat Transfer,* Part A, **28**, 253-262.

[13] Ibrahim S. Y. and Makinde O. D. (2011). Radiation effect on chemically reacting magnetohydrodynamics (MHD) boundary layer flow of heat and mass transfer through a porous vertical flat plate, *International Journal of Physical Sciences*, **6** 1508–1516.

[14] Jain Preeti and Chaudhary R. C. (2007). Hall Effect on MHD mixed convection flow of a viscoelastic fluid past an infinite vertical porous plate with mass transfer and radiation, *Ukrainian Journal of Physics,* **52(10)**, 1001-1010.

[15] Jain, Preeti and Chaudhary R. C. (2007). Combined heat and mass transfer in magneto-micropolar fluid flow from radiate surface with variable permeability in slip-flow regime, ZAMM. Z. Angew. *Math. Mech*., **87(8-9)**. 549–563.

[16] Kim Y. J. (2001). Unsteady convection flow of micropolar fluids past a vertical porous plate embedded in a porous medium, *Acta Mechanica,* **148**, 105-116.

[17] Lukaszewicz G. (1999). *Micropolar Fluids–Theory and Applications*, Birkhauser, Boston.

[18] Oahimire J. I., Olajuwon B.I., Waheed M. A. and Abiala, I. O. (2013). Analytical solution to MHD micropolar fluid flow past a vertical plate in slip-flow regime in the presence of thermal diffusion and thermal radiation, *Journal of the Nigerian Mathematical Society*, **32**, 33-60.

[19] Perdikis C. and Raptis A. (1996). Heat transfer of a micropolar fluid by the presence of radiation, *Heat and Mass Transfer*, .**31 (6),** 381-382.

[20] Rahman, M.A. and Sattar, M.A. (2007). Transient convective flow of micropolar fluid past a continuously moving vertical porous plate in the presence of radiation, *International Journal of Applied Mechanics and Engineering,* **12 (2)** 497-513.

[21] Raju M.C., Verma S.V. K., Reddy P. V. and Saha S. (2008). Soret effects due to natural convection between heated inclined plates with magnetic field, *Journal of Mechanical Engineering,* **39**, 65-70.

[22] Raptis A. and Massalas C.V. (1998). Magnetohydrodynamic flow past a plate by the presence of radiation, *Heat and Mass Transfer*, **34**, 107-109.

[23] Raptis A. A, Singh A. K. (1985). Rotation effects on MHD free-convection flow past an accelerated vertical plate, *Mechanics Research Communication*, **12(1)** 31–40.

[24] Reddy M. G. and Reddy N. B. (2010). Soret and Dufour effects on steady MHD free convection flow past a semi-infinite moving vertical plate in a porous medium with viscous dissipation, International *Journal of Applied Mathematics and Mechanics,* **6(1)**, 1-12.

[25] Sharma P. K. (2005). Fluctuating thermal and mass diffusion on unsteady free convection flow past a vertical plate in slip flow regime, *Latin American Applied Research,* .**35**, 313-319.

[26] Soundalgekar V. M. and Takhar H. S. (1983). Flow of micropolar fluid past a continuously moving plate, *International Journal of Engineering Science,* **21**, 961-965.

[27] Takhar, H. S., Chamkha, A. J. and Nath, G. (2002). MHD flow over a moving plate in a rotating fluid with magnetic field, Hall currents and free stream velocity, *International Journal of Engineering Science,* **40(13)**. 1511-1527.

[28] Takhar, H. S., Chamkha, A. J. and Nath, G. (2003). Flow and heat transfer on a stretching surface in a rotating fluid with a magnetic field, *International Journal of Thermal Sciences,* **42(1),** 23-31.

[29] Takhar H.S., Roy S. and Nath G. (2003). Unsteady free convection flow over an infinite vertical porous plate due to the combined effects of thermal and mass diffusion, magnetic field and Hall currents, Heat and Mass Transfer, **39**, 825–34.

[30] Takhar H. S. and Soundalgekar V. M. (1980). *Heat transfer in a flat plate flow of a micropolar fluid, Rheologica Acta,*.**19**,.525-526.

[31] Takhar H.S. and Soundalgekar V.M. (1985). Flow and heat transfer of micropolar fluid past a porous plate, *Indian Journal of Pure and Applied Mathematics,* **16**, 552-558.

[32] Takhar H. S. and Soundalgekar V. M. (1985). Flow and heat transfer of a micropolar fluid past a continuously moving porous plate, *International Journal of Engineering Science*, **23**, 201-205.

Acknowledgment

The First author Prof. R. C. Chaudhary is thankful to University Grants commission, New Delhi, India for awarding the Emertus Fellowship, and the second author Dr. Preeti Jain is thankful to Jagan Nath University, Jaipur, for providing necessary financial assistance.

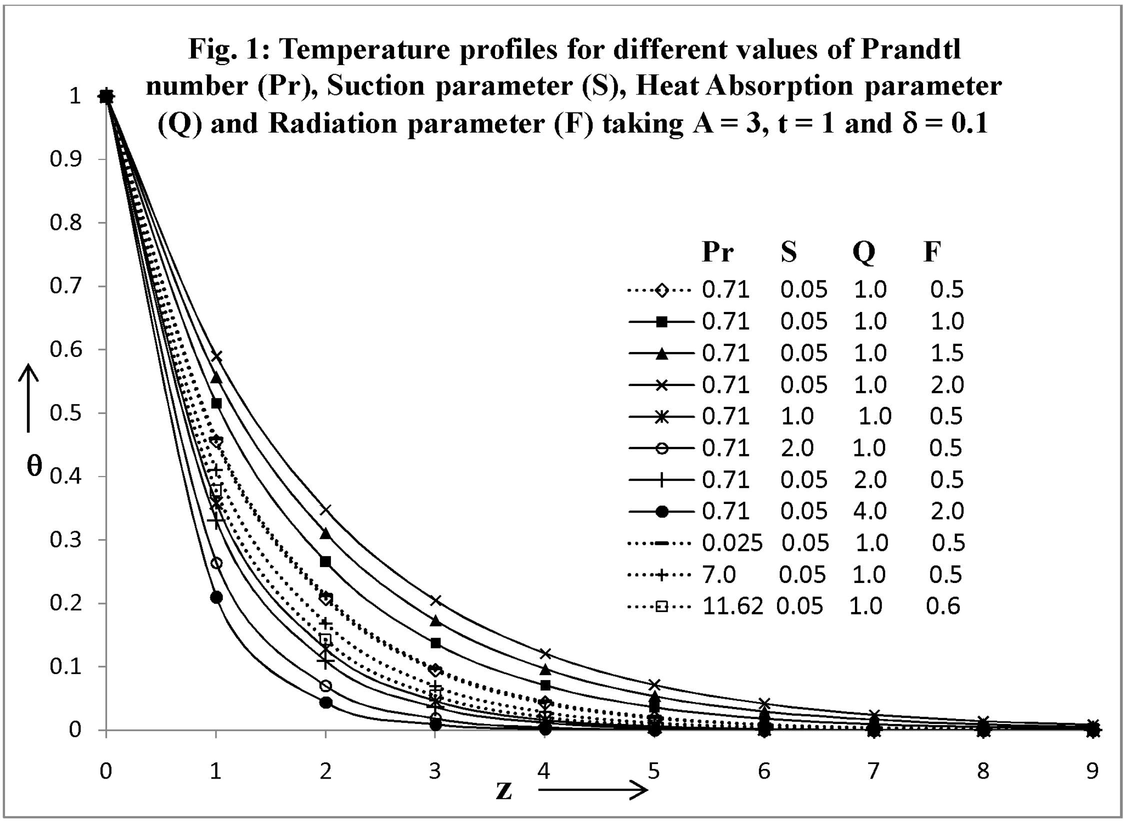

Fig. 1: Temperature profiles for different values of Prandtl number (Pr), Suction parameter (S), Heat Absorption parameter (Q) and Radiation parameter (F) taking A = 3, t = 1 and δ = 0.1

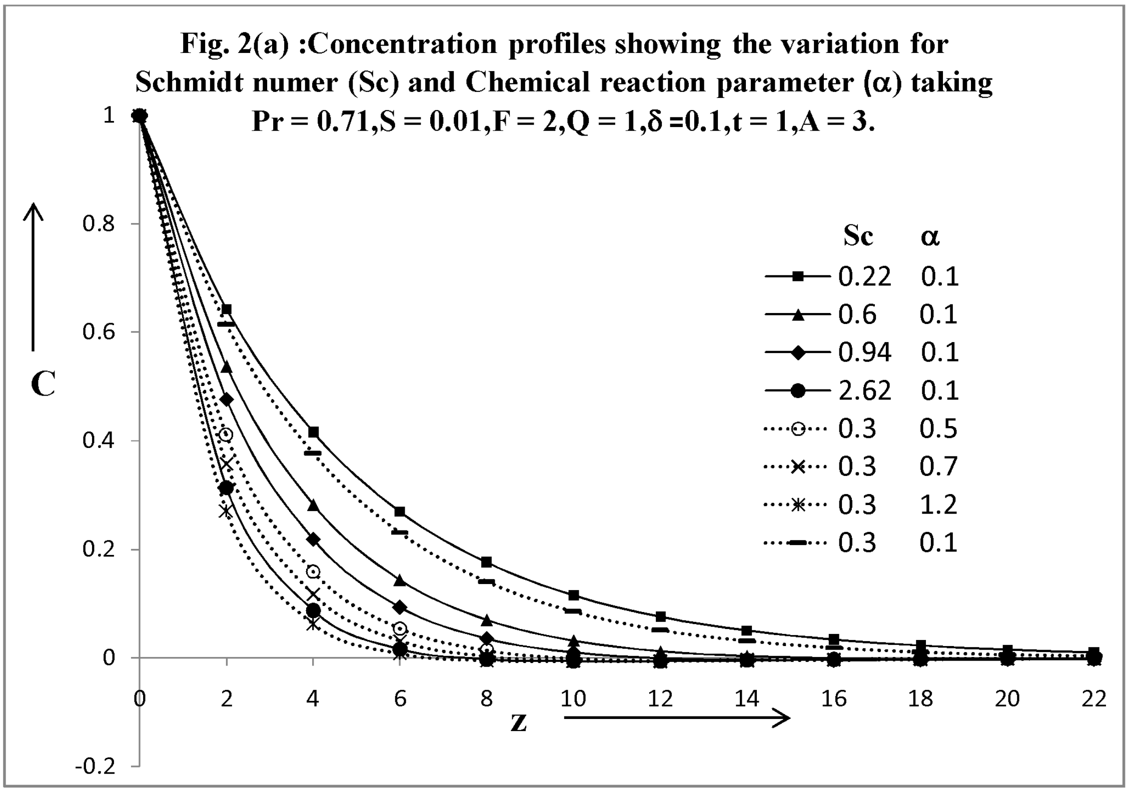

Fig. 2(a) :Concentration profiles showing the variation for Schmidt numer (Sc) and Chemical reaction parameter (α) taking Pr = 0.71,S = 0.01,F = 2,Q = 1,δ =0.1,t = 1,A = 3.

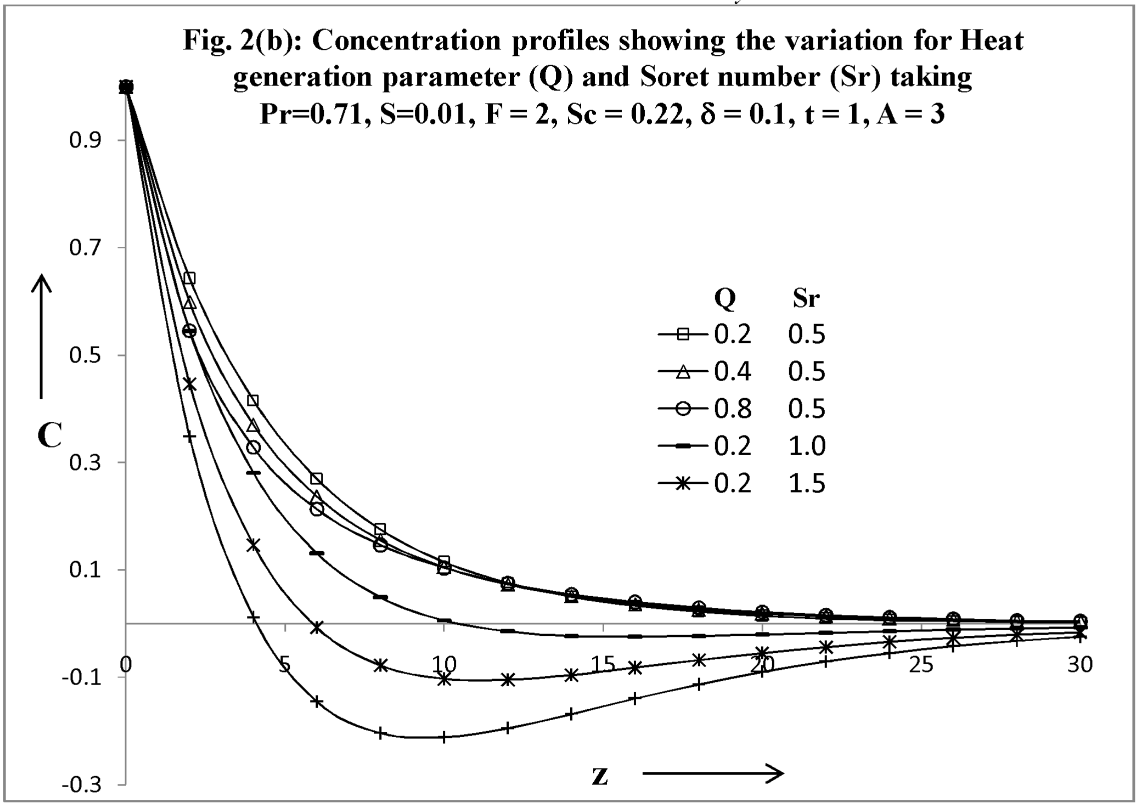
Fig. 2(b): Concentration profiles showing the variation for Heat generation parameter (Q) and Soret number (Sr) taking
Pr=0.71, S=0.01, F = 2, Sc = 0.22, δ = 0.1, t = 1, A = 3
Q Sr
0.2 0.5
0.4 0.5
0.8 0.5
0.2 1.0
0.2 1.5
C
z
0.9
0.7
0.5
0.3
0.1
-0.1
-0.3
0
5
10
15
20
25
30

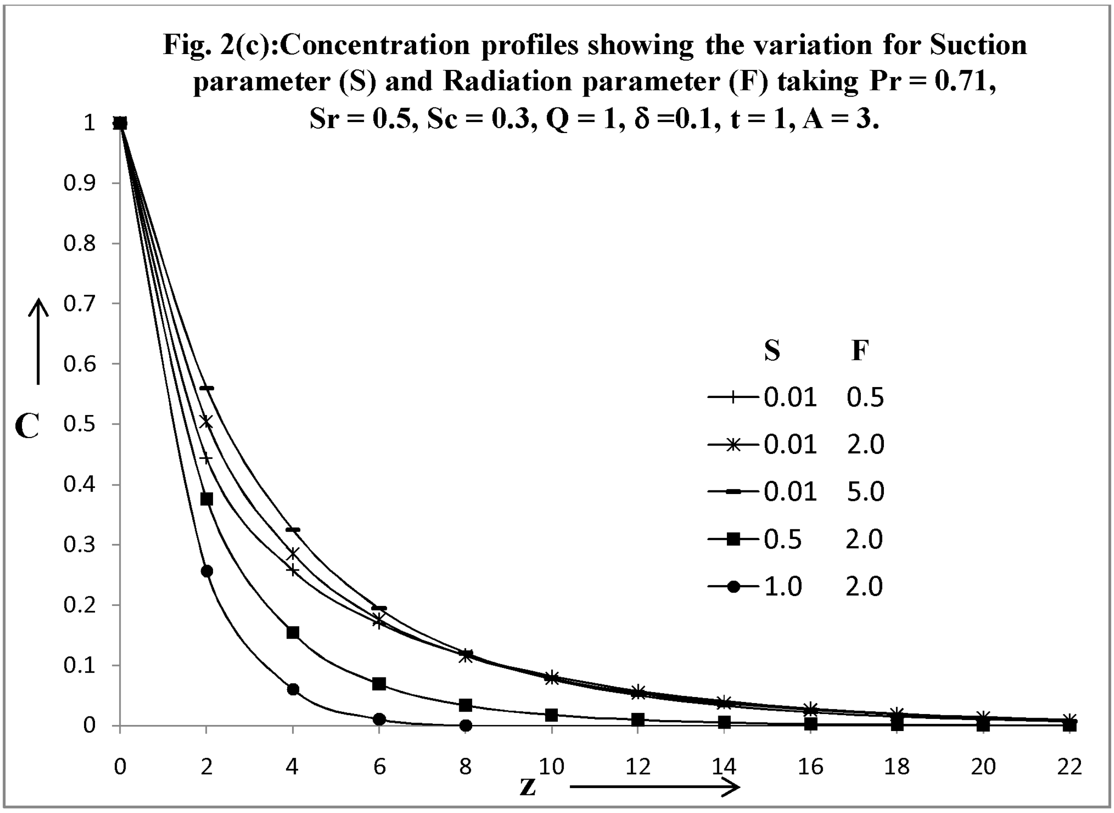
Fig. 2(c):Concentration profiles showing the variation for Suction parameter (S) and Radiation parameter (F) taking Pr = 0.71,
Sr = 0.5, Sc = 0.3, Q = 1, δ =0.1, t = 1, A = 3.
S F
0.01 0.5
0.01 2.0
0.01 5.0
0.5 2.0
1.0 2.0
C
z
1
0.9
0.8
0.7
0.6
0.5
0.4
0.3
0.2
0.1
0
0
2
4
6
8
10
12
14
16
18
20
22

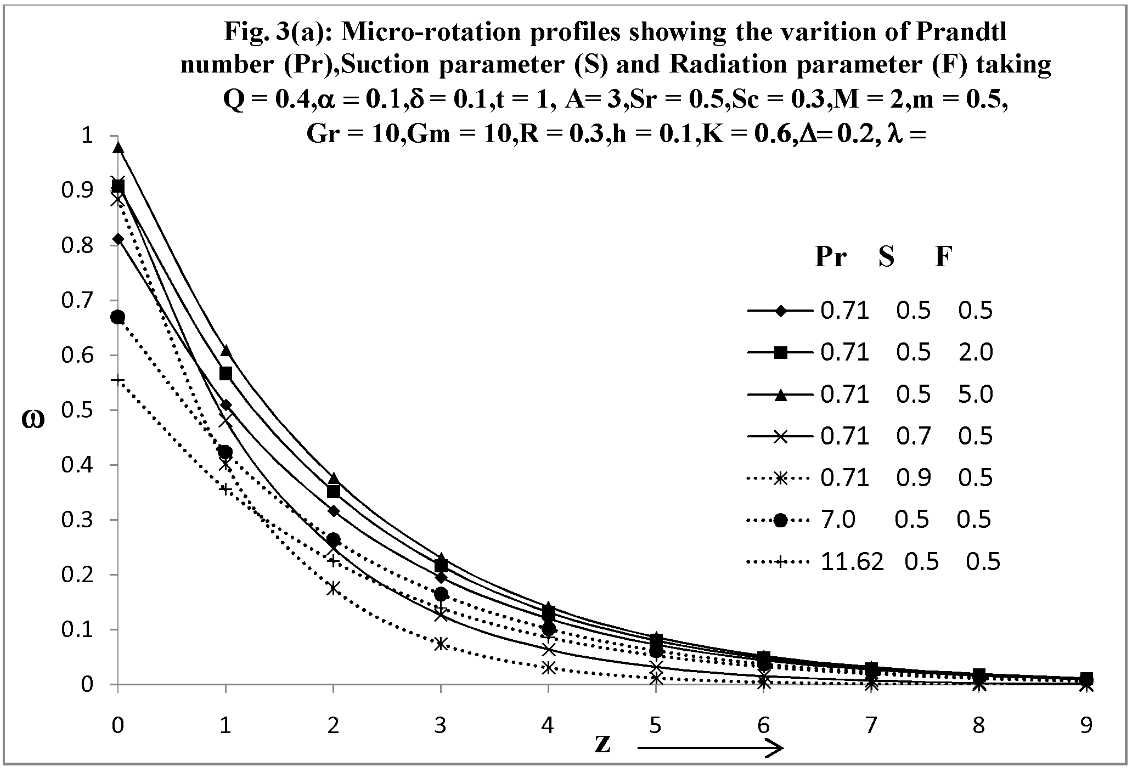

Fig. 3(a): Micro-rotation profiles showing the varition of Prandtl number (Pr),Suction parameter (S) and Radiation parameter (F) taking Q = 0.4,α = 0.1,δ = 0.1,t = 1, A= 3,Sr = 0.5,Sc = 0.3,M = 2,m = 0.5, Gr = 10,Gm = 10,R = 0.3,h = 0.1,K = 0.6,Δ= 0.2, λ =

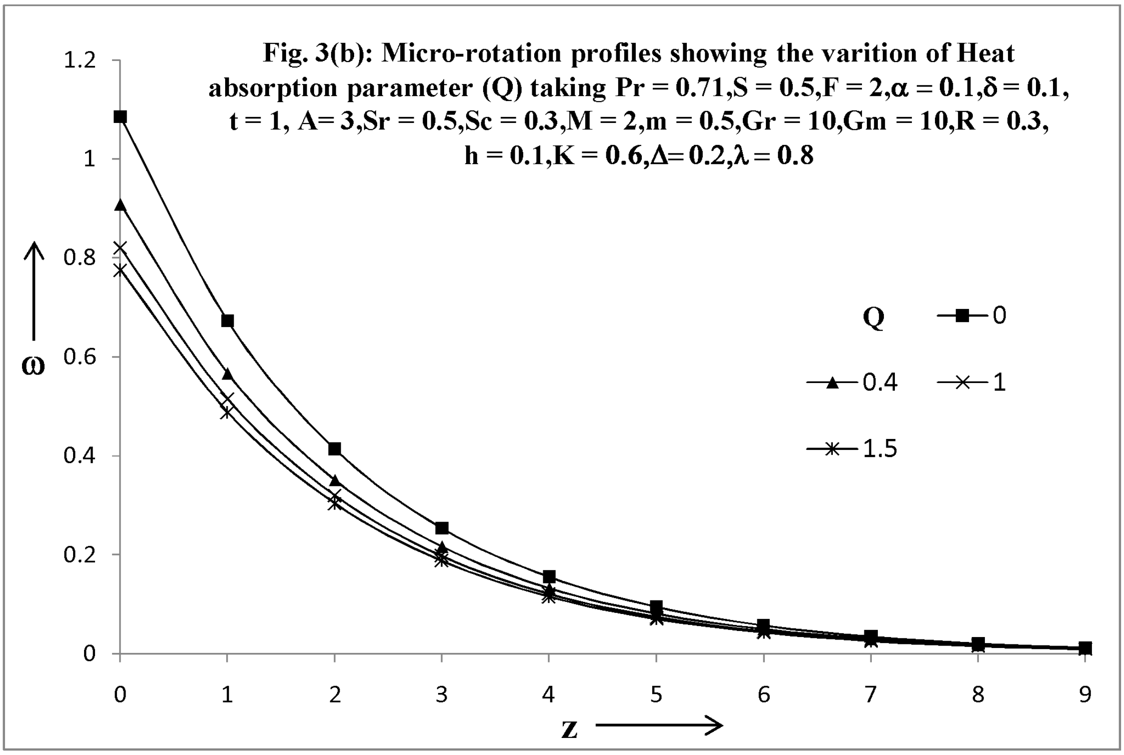

Fig. 3(b): Micro-rotation profiles showing the varition of Heat absorption parameter (Q) taking Pr = 0.71,S = 0.5,F = 2,α = 0.1,δ = 0.1, t = 1, A= 3,Sr = 0.5,Sc = 0.3,M = 2,m = 0.5,Gr = 10,Gm = 10,R = 0.3, h = 0.1,K = 0.6,Δ= 0.2,λ = 0.8

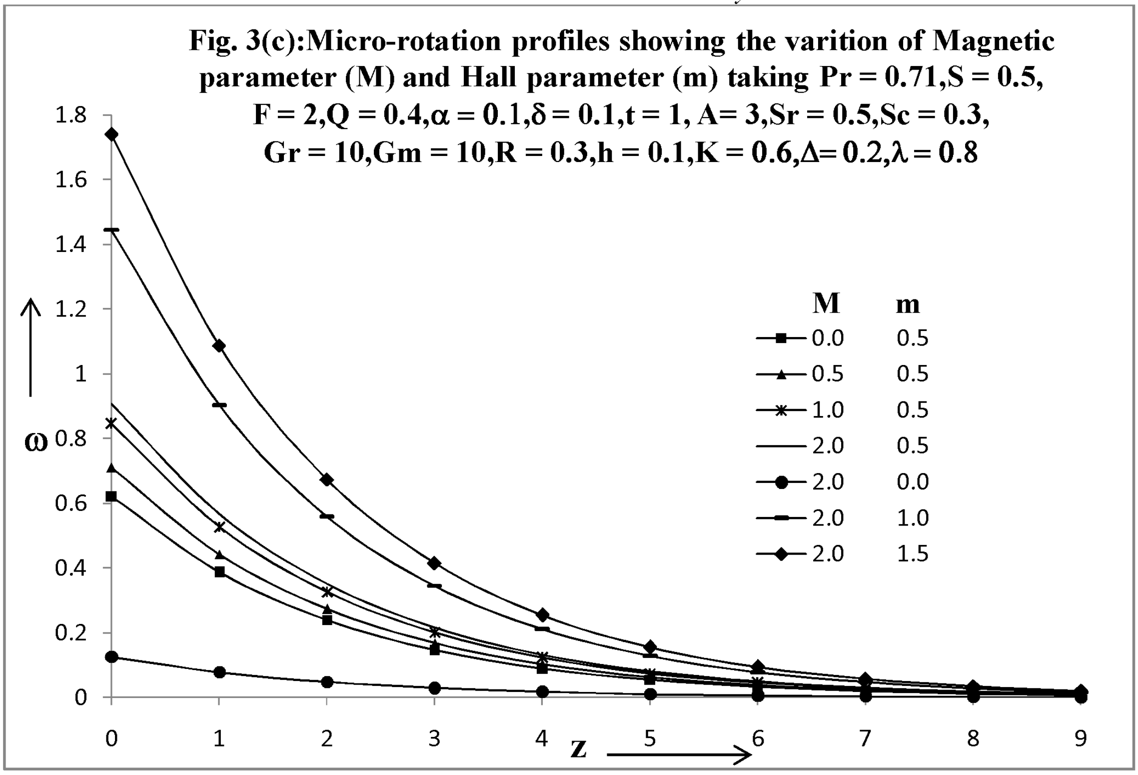

Fig. 3(c):Micro-rotation profiles showing the varition of Magnetic parameter (M) and Hall parameter (m) taking Pr = 0.71,S = 0.5, F = 2,Q = 0.4,α = 0.1,δ = 0.1,t = 1, A= 3,Sr = 0.5,Sc = 0.3, Gr = 10,Gm = 10,R = 0.3,h = 0.1,K = 0.6,Δ= 0.2,λ = 0.8

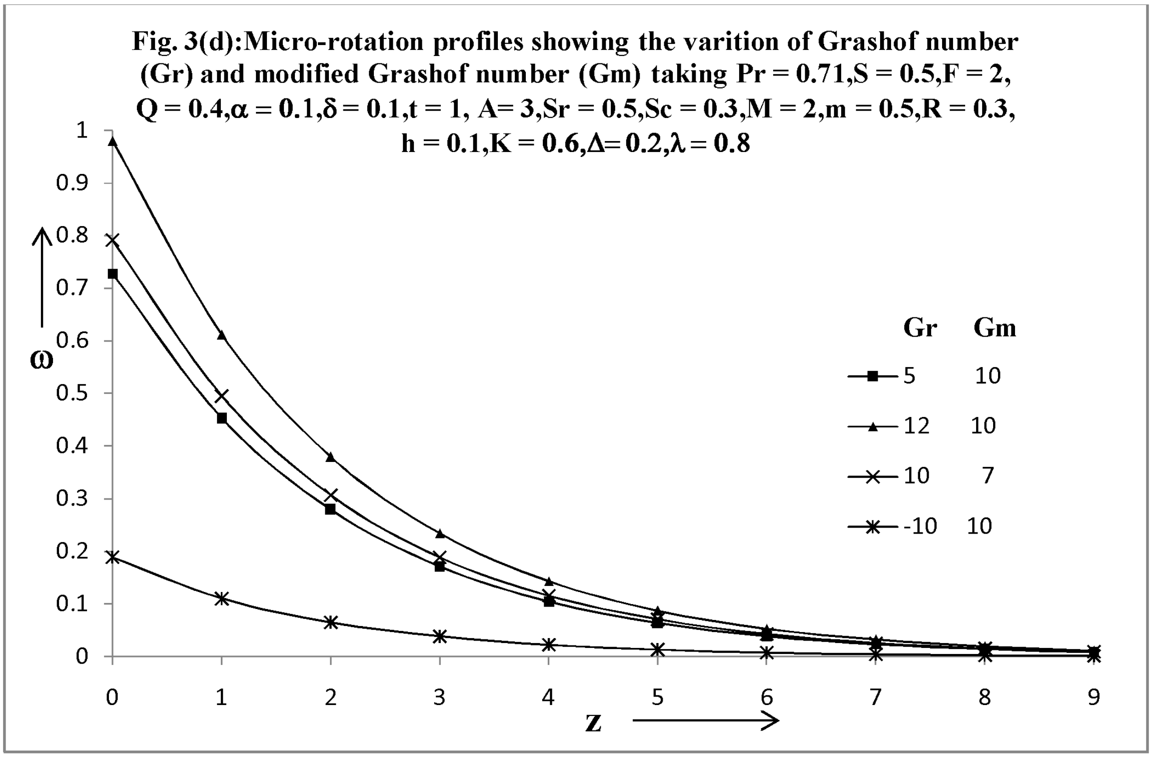

Fig. 3(d):Micro-rotation profiles showing the varition of Grashof number (Gr) and modified Grashof number (Gm) taking Pr = 0.71,S = 0.5,F = 2, Q = 0.4,α = 0.1,δ = 0.1,t = 1, A= 3,Sr = 0.5,Sc = 0.3,M = 2,m = 0.5,R = 0.3, h = 0.1,K = 0.6,Δ= 0.2,λ = 0.8

Fig. 3(e): Micro-rotation profiles showing the varition of Rotational parameter (R) taking Pr = 0.71,S = 0.5,F = 2,Q = 0.4, α = 0.1,δ = 0.1,t = 1, A= 3,Sr = 0.5,Sc = 0.3,M = 2,m = 0.5, Gr = 10,Gm = 10,h = 0.1,K = 0.6,Δ= 0.2,λ = 0.8

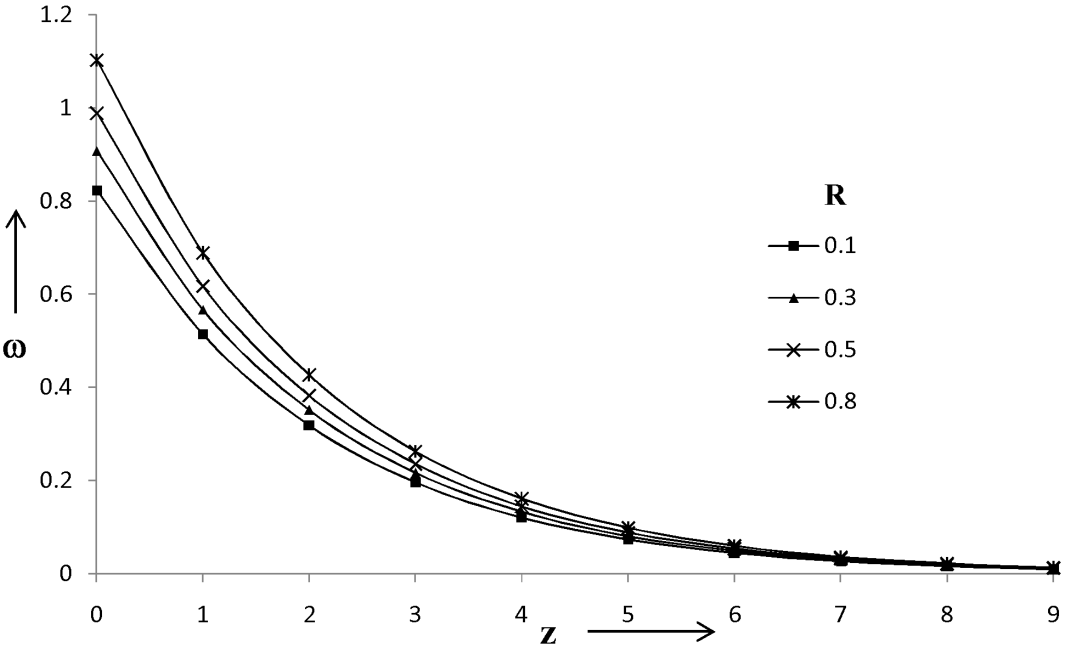

Fig. 3(f):Micro-rotation profiles showing the varition of Viscosity ratio (Δ) and Material parameter (λ) taking Pr = 0.71,S = 0.5, F = 2,Q = 0.4,α = 0.1,δ = 0.1,t = 1, A= 3,Sr = 0.5,Sc = 0.3,M = 2, m = 0.5,Gr = 10,Gm = 10,R = 0.3,h = 0.1,K = 0.6

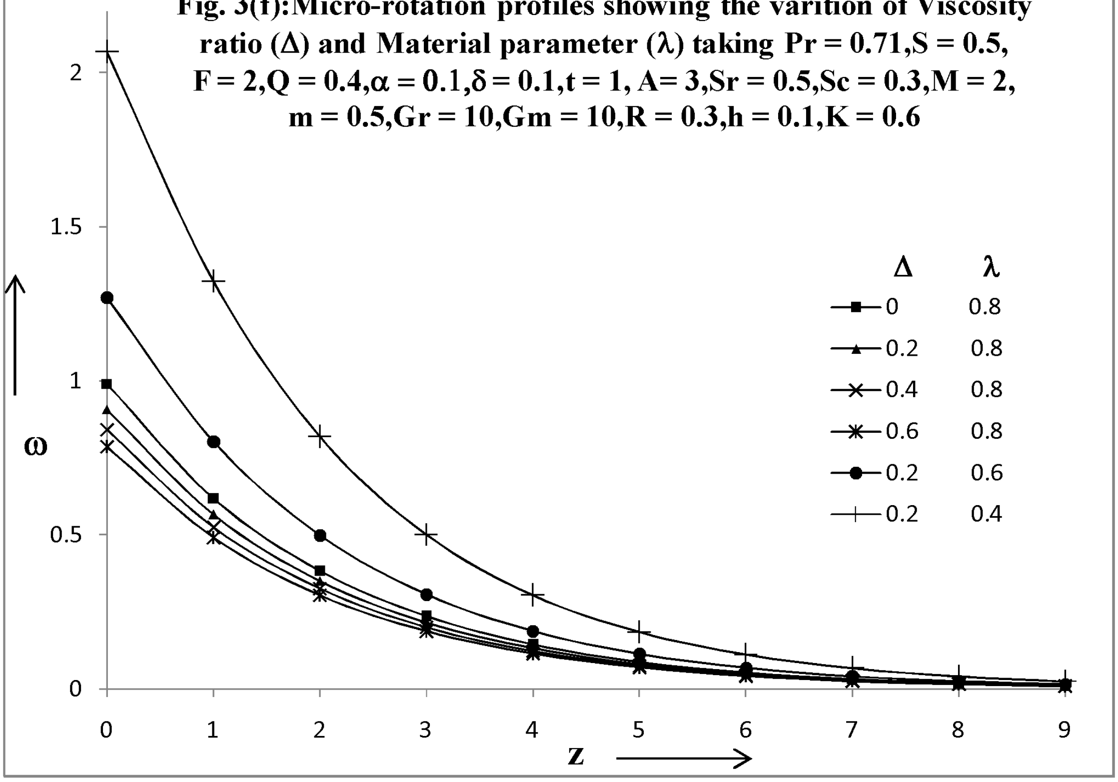

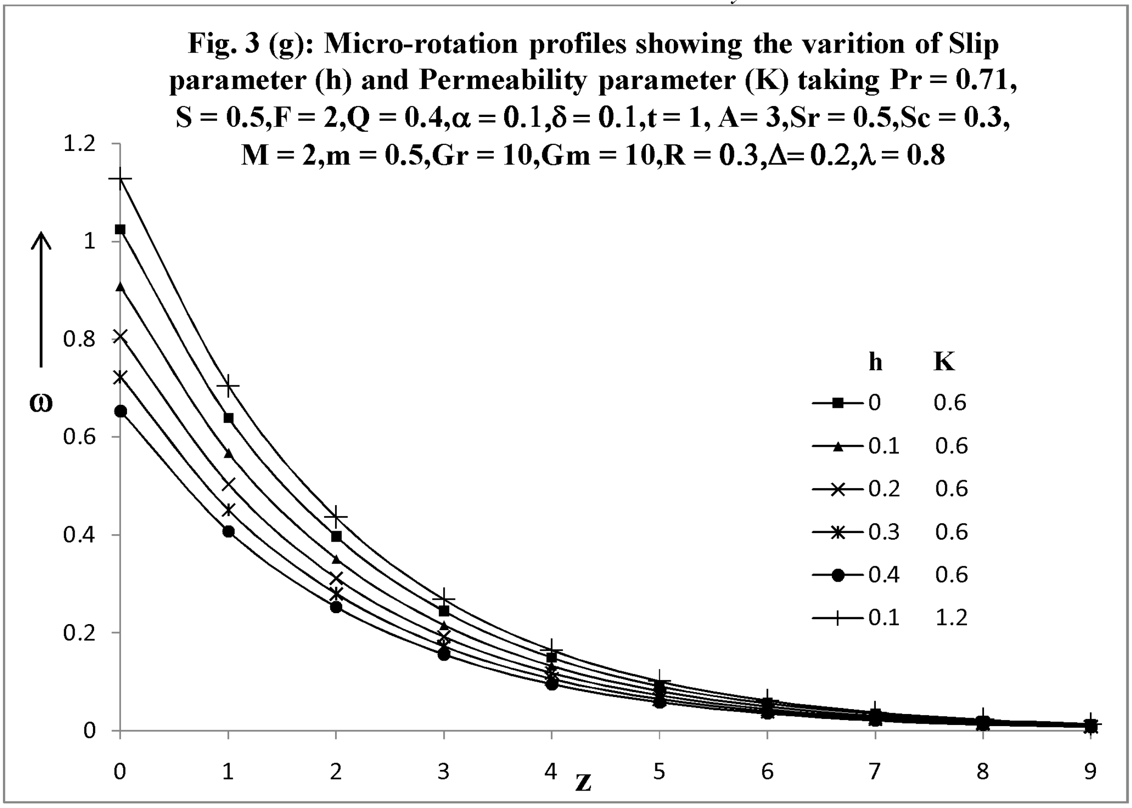

Fig. 3 (g): Micro-rotation profiles showing the varition of Slip parameter (h) and Permeability parameter (K) taking Pr = 0.71, S = 0.5,F = 2,Q = 0.4,α = 0.1,δ = 0.1,t = 1, A= 3,Sr = 0.5,Sc = 0.3, M = 2,m = 0.5,Gr = 10,Gm = 10,R = 0.3,Δ= 0.2,λ = 0.8

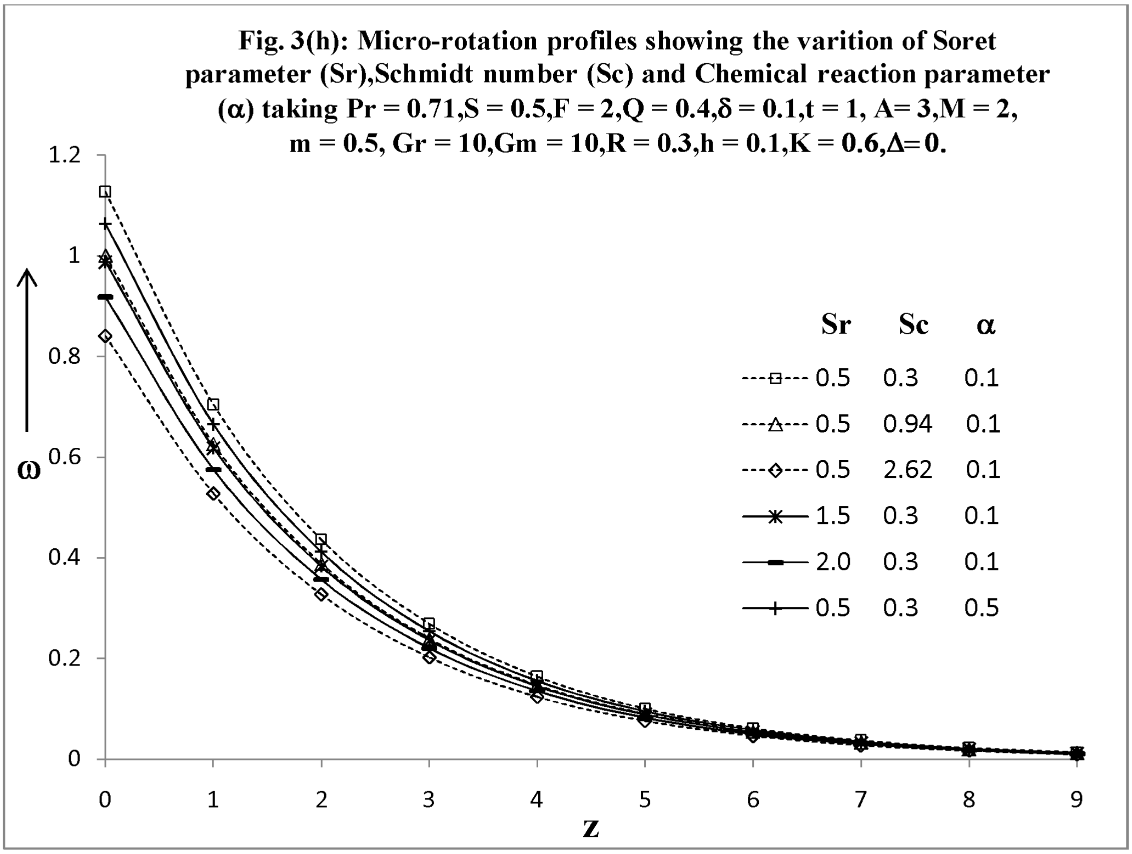

Fig. 3(h): Micro-rotation profiles showing the varition of Soret parameter (Sr),Schmidt number (Sc) and Chemical reaction parameter (α) taking Pr = 0.71,S = 0.5,F = 2,Q = 0.4,δ = 0.1,t = 1, A= 3,M = 2, m = 0.5, Gr = 10,Gm = 10,R = 0.3,h = 0.1,K = 0.6,Δ= 0.

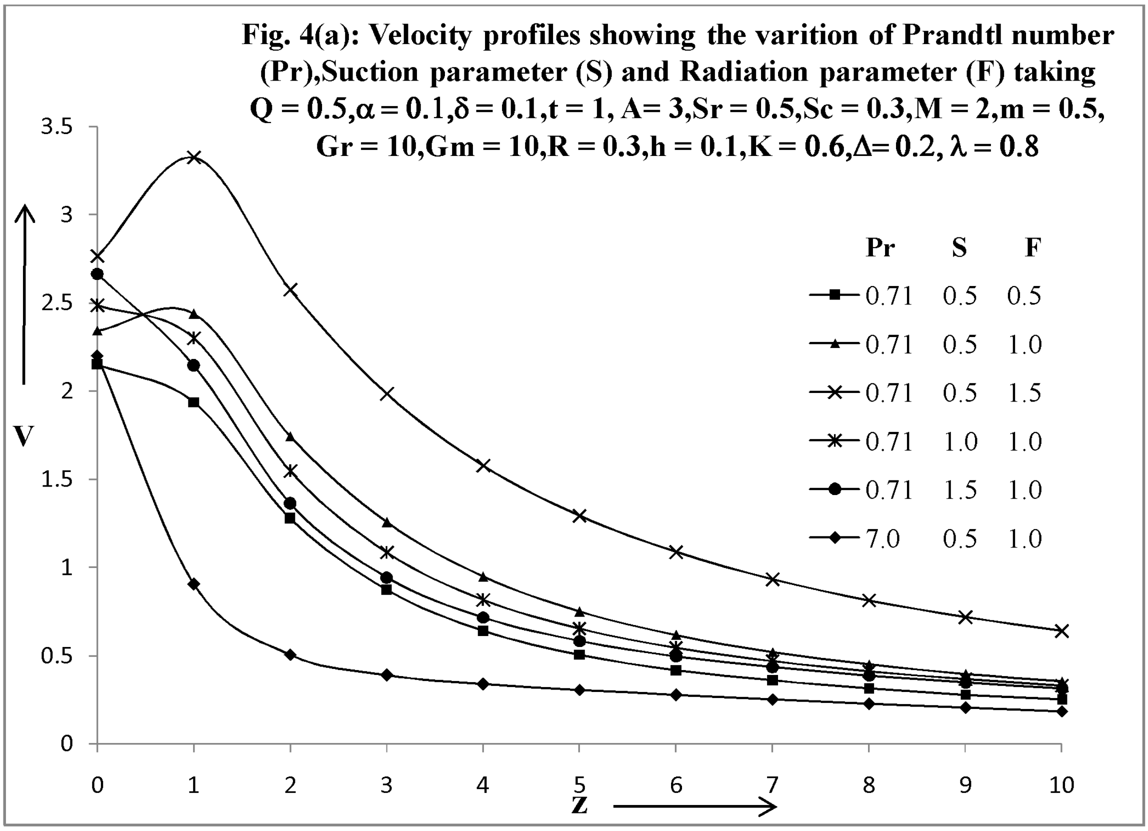
Fig. 4(a): Velocity profiles showing the varition of Prandtl number (Pr),Suction parameter (S) and Radiation parameter (F) taking Q = 0.5,α = 0.1,δ = 0.1,t = 1, A= 3,Sr = 0.5,Sc = 0.3,M = 2,m = 0.5, Gr = 10,Gm = 10,R = 0.3,h = 0.1,K = 0.6,Δ= 0.2, λ = 0.8
Pr S F
0.71 0.5 0.5
0.71 0.5 1.0
0.71 0.5 1.5
0.71 1.0 1.0
0.71 1.5 1.0
7.0 0.5 1.0
V
z
0 1 2 3 4 5 6 7 8 9 10
0 0.5 1 1.5 2 2.5 3 3.5

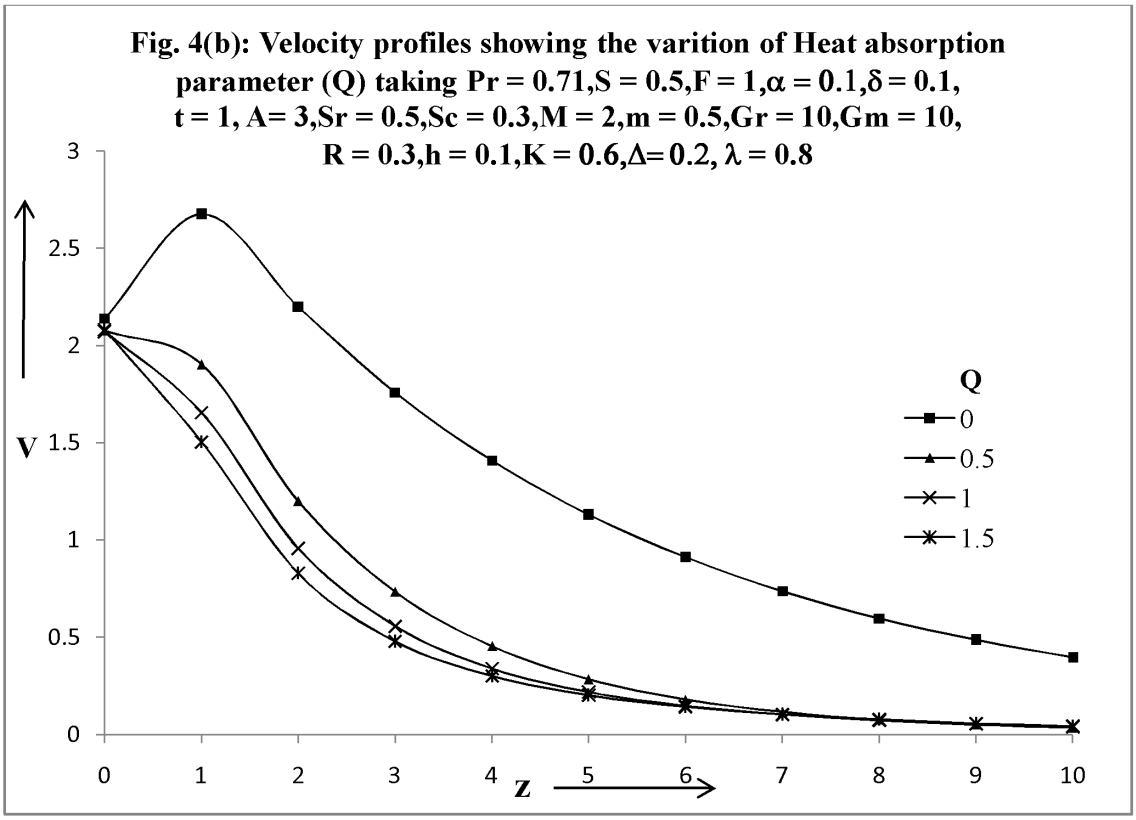
Fig. 4(b): Velocity profiles showing the varition of Heat absorption parameter (Q) taking Pr = 0.71,S = 0.5,F = 1,α = 0.1,δ = 0.1, t = 1, A= 3,Sr = 0.5,Sc = 0.3,M = 2,m = 0.5,Gr = 10,Gm = 10, R = 0.3,h = 0.1,K = 0.6,Δ= 0.2, λ = 0.8
Q
0
0.5
1
1.5
V
z
0 1 2 3 4 5 6 7 8 9 10
0 0.5 1 1.5 2 2.5 3

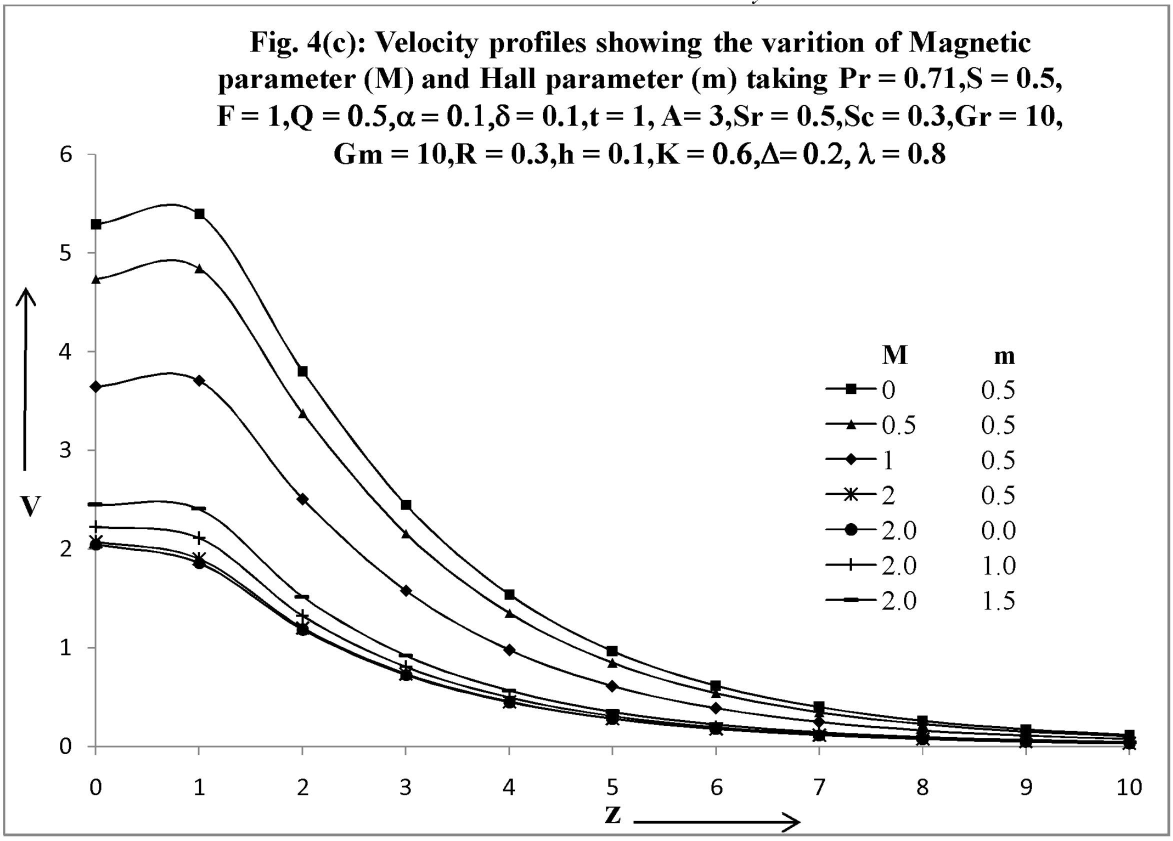

Fig. 4(c): Velocity profiles showing the varition of Magnetic parameter (M) and Hall parameter (m) taking Pr = 0.71,S = 0.5, F = 1,Q = 0.5,α = 0.1,δ = 0.1,t = 1, A= 3,Sr = 0.5,Sc = 0.3,Gr = 10, Gm = 10,R = 0.3,h = 0.1,K = 0.6,Δ= 0.2, λ = 0.8

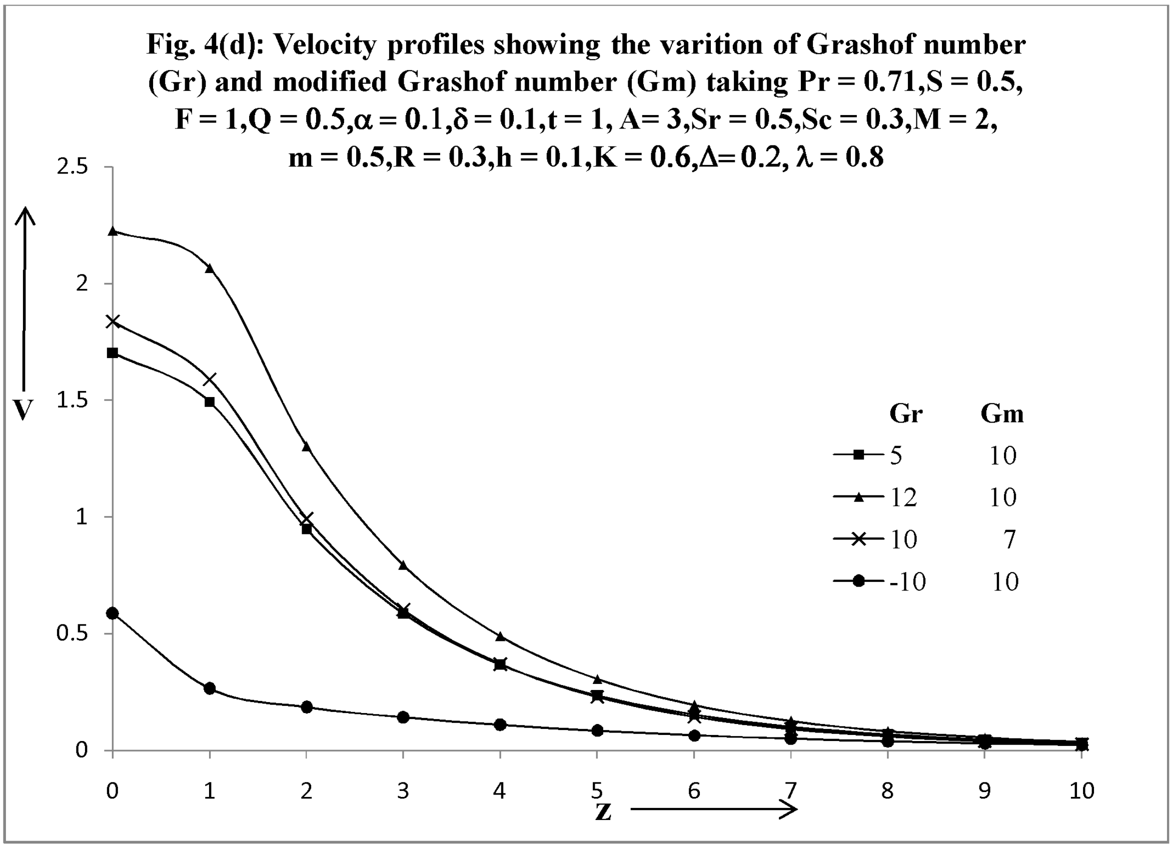

Fig. 4(d): Velocity profiles showing the varition of Grashof number (Gr) and modified Grashof number (Gm) taking Pr = 0.71,S = 0.5, F = 1,Q = 0.5,α = 0.1,δ = 0.1,t = 1, A= 3,Sr = 0.5,Sc = 0.3,M = 2, m = 0.5,R = 0.3,h = 0.1,K = 0.6,Δ= 0.2, λ = 0.8

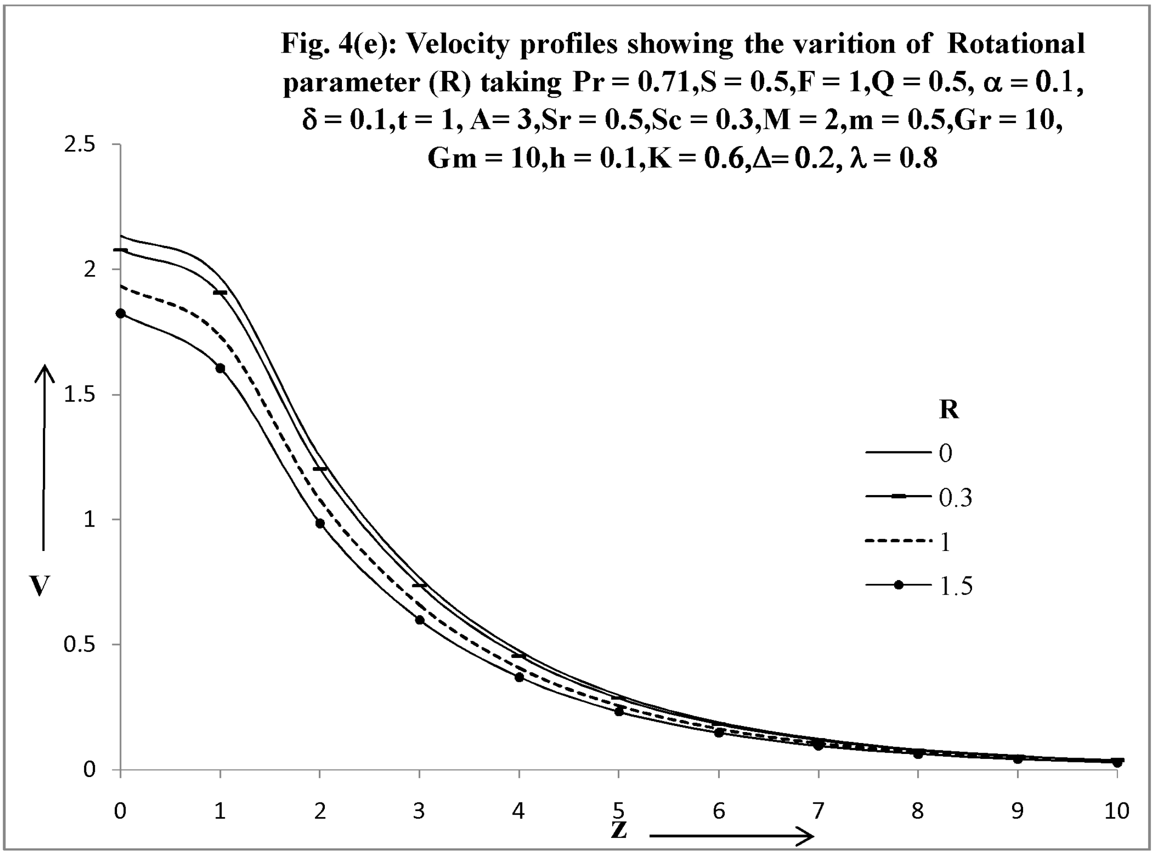

Fig. 4(e): Velocity profiles showing the varition of Rotational parameter (R) taking Pr = 0.71,S = 0.5,F = 1,Q = 0.5, α = 0.1, δ = 0.1,t = 1, A= 3,Sr = 0.5,Sc = 0.3,M = 2,m = 0.5,Gr = 10, Gm = 10,h = 0.1,K = 0.6,Δ= 0.2, λ = 0.8

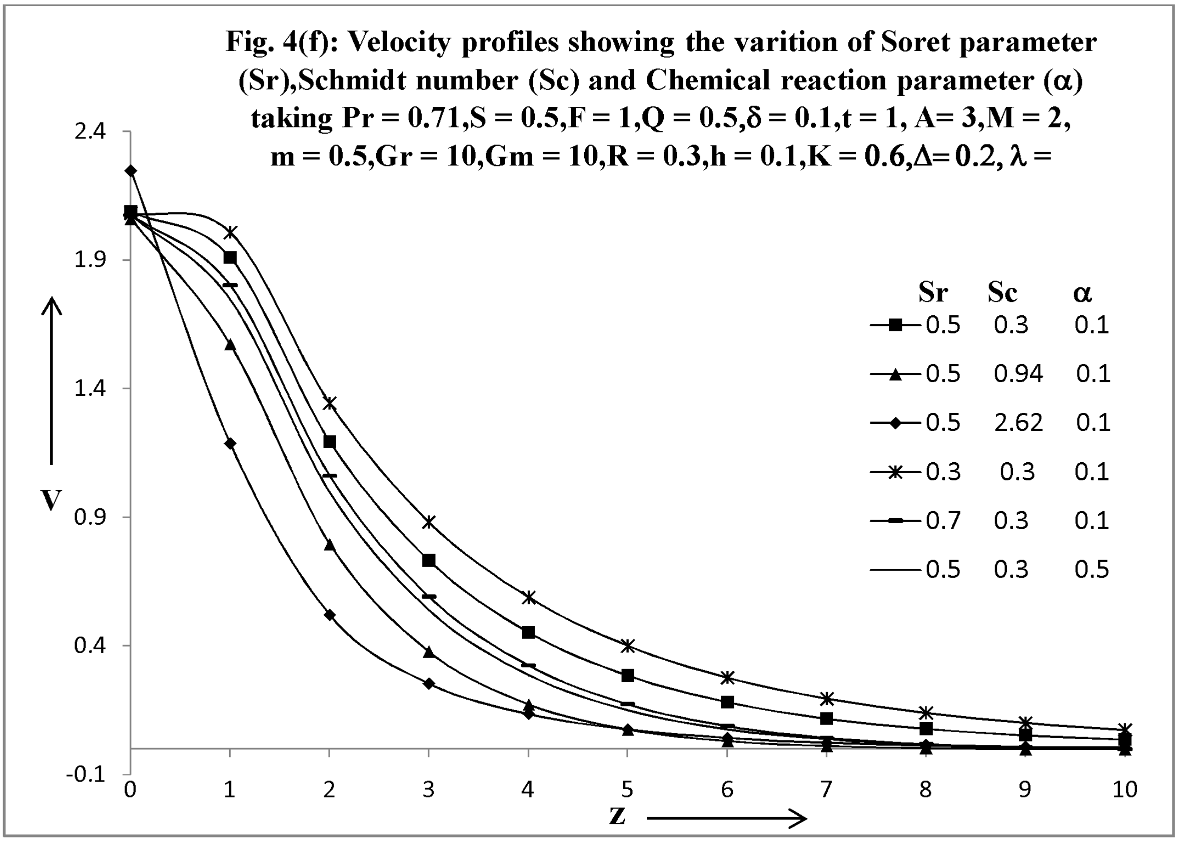

Fig. 4(f): Velocity profiles showing the varition of Soret parameter (Sr),Schmidt number (Sc) and Chemical reaction parameter (α) taking Pr = 0.71,S = 0.5,F = 1,Q = 0.5,δ = 0.1,t = 1, A= 3,M = 2, m = 0.5,Gr = 10,Gm = 10,R = 0.3,h = 0.1,K = 0.6,Δ= 0.2, λ =

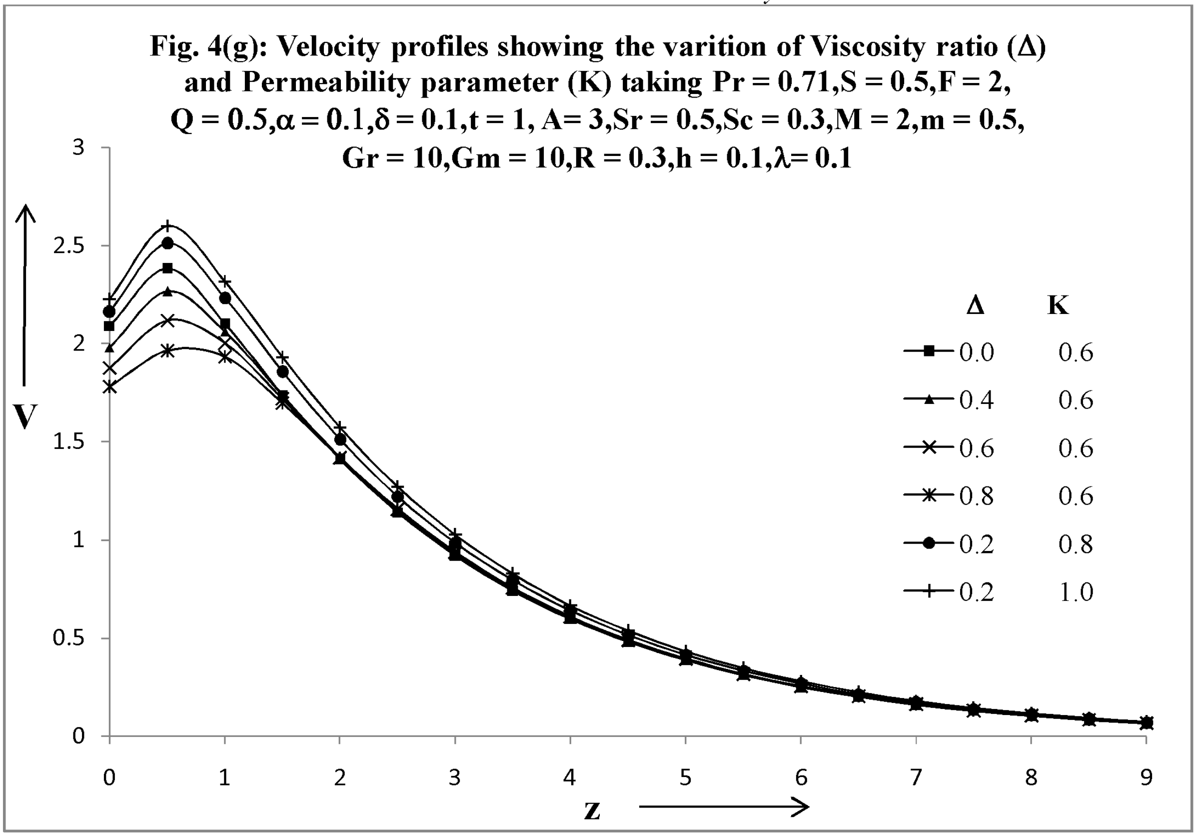

Fig. 4(g): Velocity profiles showing the varition of Viscosity ratio (Δ) and Permeability parameter (K) taking Pr = 0.71, S = 0.5, F = 2, Q = 0.5, α = 0.1, δ = 0.1, t = 1, A = 3, Sr = 0.5, Sc = 0.3, M = 2, m = 0.5, Gr = 10, Gm = 10, R = 0.3, h = 0.1, λ = 0.1

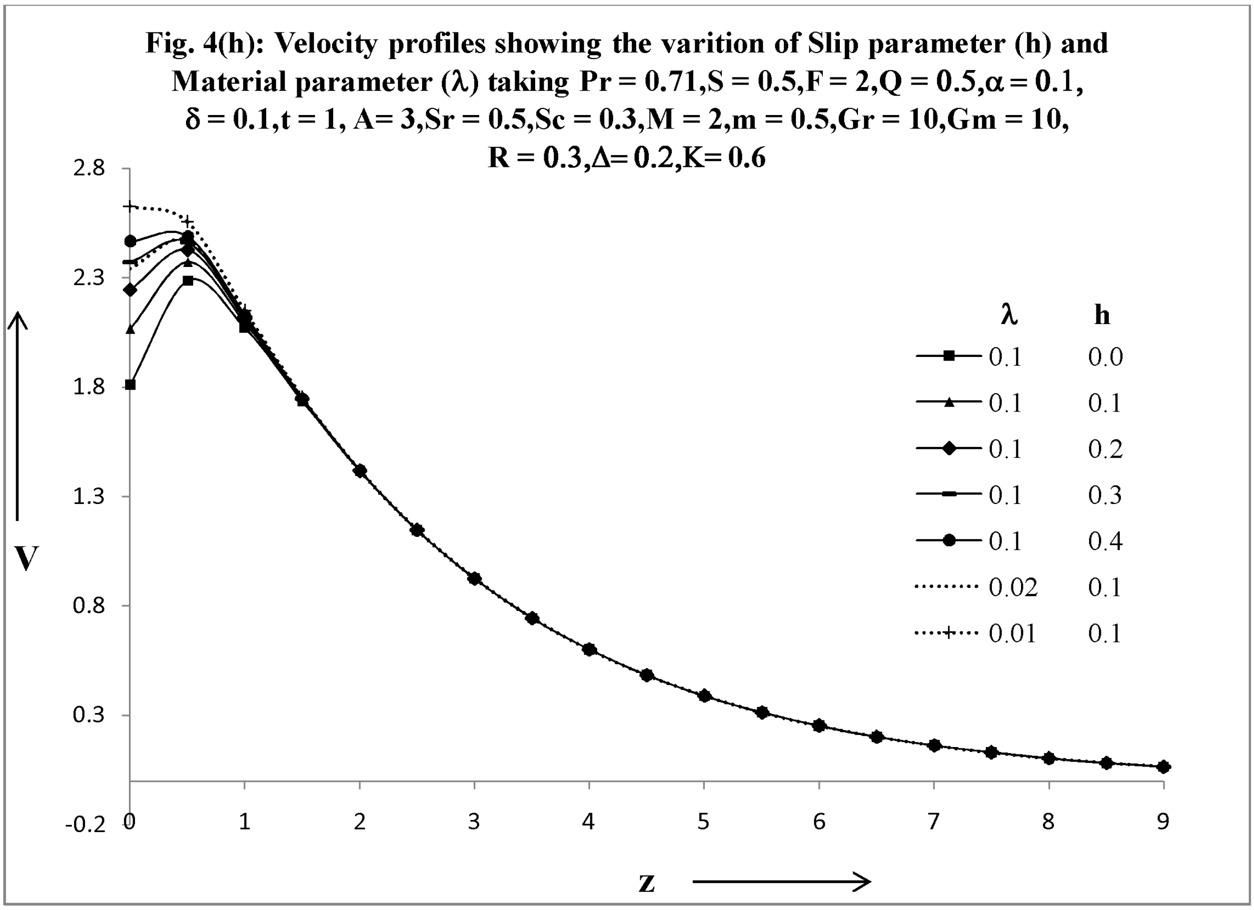

Fig. 4(h): Velocity profiles showing the varition of Slip parameter (h) and Material parameter (λ) taking Pr = 0.71, S = 0.5, F = 2, Q = 0.5, α = 0.1, δ = 0.1, t = 1, A = 3, Sr = 0.5, Sc = 0.3, M = 2, m = 0.5, Gr = 10, Gm = 10, R = 0.3, Δ = 0.2, K = 0.6